ČESKÉ VYSOKÉ UČENÍ TECHNICKÉ V PRAZE

FAKULTA STROJNÍ

ÚSTAV MATERIÁLOVÉHO INŽENÝRSTVÍ

DIPLOMOVÁ PRÁCE

Bioaktivní vrstvy na slitinách s nízkým elastickým modulem a mezivrstvou Ti deponovanou nadzvukovou kinetizací

Bioactive coatings on low elastic modulus alloys and Ti bond layer by cold kinetic spray

AUTOR: Vojtěch Lukeš

STUDIJNÍ PROGRAM: Výrobní inženýrství

VEDOUCÍ PRÁCE: doc. Ing. Jan Čížek Ph.D.

PRAHA 2023

ZADÁNÍ DIPLOMOVÉ PRÁCE

I. OSOBNÍ A STUDIJNÍ ÚDAJE

Příjmení: **Lukeš** Jméno: **Vojtěch** Osobní číslo: **482590**

Fakulta/ústav: **Fakulta strojní**

Zadávající katedra/ústav: **Ústav materiálového inženýrství**

Studijní program: **Výrobní inženýrství**

Specializace: **Bez specializace**

II. ÚDAJE K DIPLOMOVÉ PRÁCI

Název diplomové práce:

Bioaktivní vrstvy na slitinách s nízkým elastickým modulem a mezivrstvou Ti deponovanou nadzvukovou kinetizací

Název diplomové práce anglicky:

Bioactive coatings on low elastic modulus alloys and Ti bond layer by cold kinetic spray

Pokyny pro vypracování:

1. Vypracovat rešerši o materiálech pro implantáty kostní tkáně, a základních charakteristikách technologií studené kinetizace a plazmového stříkání z kapalin.
2. Provést depozici vrstev Ti na zvolený podkladový materiál pomocí studené kinetizace.
3. Provést depozici vrstev hydroxylapatitu plazmovým nanášením ze suspenzí na vrstvu Ti.
4. Provést mikrostrukturní analýzu vyhotovených vrstev.

Seznam doporučené literatury:

1. Papyrin, Kosarev, Klinkov, Alkhimov, Fomin: Cold Spray Technology. Elsevier Science, 2006.
2. Heimann, Lehmann: Bioceramic coatings for medical implants. Wiley, 2015.
3. Wang, Zhang: Cold-spray coatings on magnesium and its alloys. Surface Modification of Magnesium and its Alloys for Biomedical Applications. Woodhead Publishing, 2015.
4. Cizek, Brozek, Chraska, Lukac, Medricky, Musalek, Tesar, Siska, Antos, Cupera, Matejkova, Spotz, Houdkova, Kverka: Silver-doped hydroxyapatite coatings deposited by suspension plasma spraying. Journal of Thermal Spray Technology, 27, 2018, 1333.

Jméno a pracoviště vedoucí(ho) diplomové práce:

doc. Ing. Jan Čížek, Ph.D. Ústav materiálového inženýrství

Jméno a pracoviště druhé(ho) vedoucí(ho) nebo konzultanta(ky) diplomové práce:

Datum zadání diplomové práce: **23.03.2023** Termín odevzdání diplomové práce: **31.07.2023**

Platnost zadání diplomové práce: _____

doc. Ing. Jan Čížek, Ph.D. podpis vedoucí(ho) práce	doc. Ing. Ladislav Cvrček, Ph.D. podpis vedoucí(ho) ústavu/katedry	doc. Ing. Miroslav Španiel, CSc. podpis děkana(ky)

III. PŘEVZETÍ ZADÁNÍ

Diplomant bere na vědomí, že je povinen vypracovat diplomovou práci samostatně, bez cizí pomoci, s výjimkou poskytnutých konzultací. Seznam použité literatury, jiných pramenů a jmen konzultantů je třeba uvést v diplomové práci.

Datum převzetí zadání Podpis studenta

Prohlášení

Prohlašuji, že jsem tuto práci vypracoval samostatně, a to výhradně s použitím pramenů a literatury uvedených v seznamu citovaných zdrojů.

V Praze dne: …… ……..

Podpis

Anotace

Tato diplomová práce pojednává o využití technologií cold spray a WSP-H pro depozici hybridního povlaku složeného z krycí mezivrstvy titanu a svrchní vrstvy hydroxylapatitu na substrát z hořčíkové slitiny. Cílem experimentu je určit, zda je možné takový duplexní povlak deponovat a následně vyhodnotit jeho vlastnosti, jako je tloušťka, porozita a chemické složení. Tato studie vznikla ve spolupráci s Ústavem fyziky plazmatu Akademie věd České republiky.

Klíčová slova

Biomateriály, hořčík, titan, hydroxylapatit, cold spray, plazmové nanášení

Annotation

This master's thesis focuses on the utilization of cold spray and WSP-H technologies for depositing a hybrid coating composed of a titanium interlayer and a top layer of hydroxyapatite onto a magnesium alloy substrate. The objective of the experiment is to determine the feasibility of depositing such coating and subsequently evaluate its properties, such as thickness, porosity, and chemical composition. The study was conducted in collaboration with the Institute of Plasma Physics of the Czech Academy of Sciences.

Keywords

Biomaterials, magnesium, titanium, hydroxylapatite, cold spray, plasma spray

Poděkování

Děkuji především vedoucímu mé diplomové práce doc. Ing. Janu Čížkovi Ph.D. za trpělivý, odborný přístup a cenné rady. Svým rodičům a bratrovi děkuji za podporu během celé délky studia. Dále děkuji kolegům z Politecnico di Milano v Itálii (prof. Sara Bagherifard, prof. Mario Guagliano) za umožnění depozice technologií cold spray a Ing. Janu Medřickému Ph.D. za depozici vrstvy hydroxylapatitu.

Table of contents

1 Introduction

Throughout recent history, the pursuit of improved reliability in hard tissue replacements has driven the development and utilization of various metallic materials. These include ferrous, cobalt-chromium-based, and titanium-based alloys. However, a significant drawback of these alloys is their relatively high elastic moduli, in comparison to that of human bones. Consequently, upon implantation, these materials may give rise to undesirable phenomena and potentially lead to implant failure.

To address this issue, there is a growing need to explore a new generation of implants that employ alloys with low elastic modulus. Among the promising options, magnesium alloys have gained attention. However, the use of these alloys presents an additional challenge, as they do not inherently possess full biocompatibility. When interacting with the human body, magnesium alloys are highly susceptible to corrosion and can release harmful alloying elements. Thus, to enable their application, it becomes necessary to protect and shield the alloy surfaces from the corrosive environment through the implementation of surface layers.

The primary objective of this thesis is to investigate the potential implementation of bioactive coatings composed of two layers (a base shielding layer and a more bioactive top layer) on low elastic modulus alloys. The initial literature review section examines the concept of biocompatibility in materials designed for hard tissue replacements and explores their practical applications. Subsequently, an overview of coating technologies is provided, with emphasis on cold spray and plasma spray techniques as the two methods used in our study.

The experimental part of this research involves depositing a hybrid cold spray/plasma spray coating onto a magnesium AZ31 substrate. The subsequent evaluation of the microstructure, porosity and chemical composition confirms the feasibility of applying a cold sprayed titanium base layer with a hydroxylapatite top layer deposited from suspension using the WSP-H process and thus enhancing the biocompatibility of the magnesium alloy.

2 Literature review

In the first part of this chapter, the concept of biocompatibility is explained, followed by information on nowadays biomaterials. Coating technologies are then introduced in the second part, with special emphasis on the two methods employed in this study.

2.1 Biocompatibility

Biocompatibility is a fundamental requirement for the successful integration of synthetic implants within the human body. It encompasses the ability of the surrounding tissue and the entire biological system to accept these implants without triggering undesirable immune responses, allergic reactions, inflammatory complications, or chronic issues. Achieving biocompatibility ensures optimal relationship between the implanted material and the biological environment, allowing for sustained functionality and long-term performance of the implant [1].

Several key considerations are involved in assessing biocompatibility, including the interaction with the surroundings (cytotoxins, toxicological or allergic reactions, carcinogenic or mutagenic reactions, inflammatory processes, biodegradation), the duration of implant application (long-term or short-term), surface biocompatibility (chemical, biological, and morphological suitability), structural biocompatibility (adaptability of implant's mechanical properties to host tissue), function (friction coefficient, mechanical properties for the intended application), and material (aggressiveness of the synthetic material to the host tissue and vice versa) [1].

If a material complies with all the requirements considering biocompatibility, it can be labeled as a biomaterial. Based on the material's response to the environment of the human body, they are further divided into bioinert, bioactive and bioresorbable biomaterials.

Bioinert materials refer to substances that exhibit minimal reactivity with the surrounding tissue when introduced into the body. The surrounding tissues encapsulate the bioinert implant with connective tissue, thereby integrating it with the body only via a mechanical connection. Common examples of bioinert materials include chrome steel, titanium, alumina, partially stabilized zirconia, and ultra-high molecular weight polyethylene [1].

Bioactive biomaterials can induce a specific tissue response, improving integration with the surrounding biological system. In hard tissue implants, they can be categorized as osteoconductive or osteoproductive. Osteoconductive biomaterials bond to hard tissues and promote tissue interaction on their surface, while osteoproductive biomaterials stimulate the growth of new tissue away from the biomaterial interface.

Bioresorbable biomaterials undergo time-dependent controlled degradation, allowing them to be gradually replaced by host tissue. However, for practical use, it is crucial for a resorbable biomaterial to be metabolically acceptable due to the significant amount of degraded material that will be handled by the tissues. Additionally, the rate of resorption must be appropriately matched to the repair rates of the host's biological tissue. When utilizing bioresorbable biomaterials in a clinical context, it is essential to ensure that the mechanical properties of the biomaterial support tissue repair. Magnesium implants are an example of such bioresorbable biomaterials [1].

2.2 Biomaterials

Another, more common categorization of biomaterials is based on the type of materials, which includes ceramics, metals, polymers, and composites.

2.2.1 Ceramics

Bioceramics are a class of inorganic, nonmetallic materials that are known for their superior compressive strength and biocompatibility, making them useful in medical applications. The selection of a specific bioceramic depends upon the desired method of tissue attachment. Dense, inert ceramics such as Al_2O_3 and ZrO_2 achieve the attachment through bone ingrowth. In the case of surface features and irregularities with sizes exceeding 100 µm, biological fixation occurs as bone ingrowth anchors the material securely. Reactive ceramics like calcium phosphates form chemical bonds directly with the bone, thus ensuring a firm connection. Bioglass and resorbable ceramics gradually dissolve, synchronizing with the rate of new bone formation. Notably, certain compositions of bioactive glass, including those within the SiO_2–CaO–Na_2O–P_2O_5 system, exhibit the ability to bond with soft tissues, further expanding their applications [2].

Probably the most prominent calcium phosphate compound is hydroxylapatite. With the composition of $Ca_{10}(PO_4)6(OH)_2$ it constitutes approximately 69 % (by volume) of the mineral component in human bone. It is the most stable calcium phosphate polymorph under physiological conditions and exhibits significant biological activity, promoting bone growth and integration without degradation or dissolution. While its mechanical properties as a bulk material are insufficient for major load-bearing devices, depositing a bioactive thin film of HA onto bio-inert implants has seen successful clinical usage [3].

2.2.2 Metals

Metals are highly favored for their suitability in long-term, durable, and load-bearing implants due to their strength and ductility, resulting in a high resistance to fracture. Moreover, the versatility of metal implants allows to produce complex architectures using various manufacturing methods such as casting, machining, and powder metallurgy. Two critical factors

for successful implants are their biocompatibility and ability to match the mechanical properties of the bone [4].

Considering the effects of corrosion and wear is crucial when assessing the biocompatibility of metallic implants. The release of harmful metal ions resulting from these processes can trigger inflammatory responses, cell apoptosis, and other adverse tissue reactions. Chromium (in Co-Cr alloys), aluminum, vanadium, and nickel (in Ti-based alloys) are among the ions that have been linked to detrimental tissue reactions when their concentration in tissues or body fluids exceeds certain limits. Nickel, for example, has been identified as a highly cytotoxic, genotoxic, carcinogenic, and mutagenic element. Furthermore, most metals exhibit relatively limited bioactivity, which can affect their long-term functionality and integration within the biological system [4]. Commonly used materials for prosthetic applications include ferrous alloys (such as austenitic stainless steel 316L), titanium alloys (such as Ti6Al4V and Ti6Al7Nb, Ti29Nb13Ta4.6Zr), cobalt-chromium alloys (such as Co28Cr6Mo and Co20Cr15W) and magnesium alloys (such as Mg6Zn, AZ51, and AZ91) [1].

316L, an austenitic stainless steel, is frequently used in bone replacements, but its Young's modulus and tensile strength are about ten times higher than those of human bone. This can lead to the stress shielding effect, in which the implant bears too much load, preventing the surrounding tissue from carrying enough stress, resulting in bone cell death and the implant failure. Additionally, the presence of Cr and Ni ions can cause cytotoxicity [1]. Co28Cr6Mo is another widely used alloy, but like 316L, it has concerns about biocompatibility and high Young’s modulus. It does offer better corrosion and wear resistance compared to 316L [5].

Titanium alloys have mechanical properties that are more similar to bone, including a lower Young's modulus (110-118 GPa), higher fatigue strength, and better corrosion resistance compared to stainless steel and CoCr alloys. For this reason, titanium dental implants are a viable option (Figure 1). However, one of the main challenges of titanium alloys is their low wear resistance, which can be problematic in load-bearing joint implants, where abrasive wear is common. Despite this, titanium alloys tend to elicit a more favorable response from the surrounding tissue, leading to research of ways to improve the wear resistance through depositing abrasion resistant coatings with techniques such as cold spray or thermal spray. The most commonly used titanium alloys currently are Ti6Al4V, Ti6Al7Nb, and Ti5Al2.5Fe, but due to the toxicity of elements such as Al and V, newer alloys such as Ti45Nb, Ti30Ta, and Ti29Nb13Ta4.6Zr are considered more suitable for implant materials [4].

Magnesium possesses advantageous characteristics that make it a viable choice in orthopedics. The corrosion products of magnesium are believed to have more physiological benefits than harm. It is important to note that the adult human body naturally contains approximately 30 g of magnesium. Magnesium, along with calcium, sodium, and potassium, is efficiently regulated by homeostatic mechanisms in the body, reducing the risk of toxicity as the body can handle as much as 400 g of magnesium. Consequently, adverse effects or poisoning from magnesium are generally rare [6].

With a specific density of approximately 1.7 g/cm³, magnesium and its alloys closely resemble the density of human calvarium bone (1.75 g/cm³). Moreover, the elastic modulus of pure magnesium, around 45 GPa, aligns well with that of human bone (40-57 GPa) which mitigates the stress shielding effect and relative motion between an implant and the bone [7].

However, Mg has a high degradation rate in Cl- containing solutions due to its low standard reduction potential, which leads to the evolution of hydrogen and the formation of degradation products on the surface of the alloy, causing further dissolution of the metal [6]. This unfortunate characteristic of magnesium could be solved by shielding the surface with another metal with more favorable bioinert properties.

Studies have showcased promising results, such as the use of magnesium scaffolds (e.g., AZ91) as subchondral bone replacements for cartilage repair. In vivo investigations have provided evidence of new bone formation and biocompatibility following the implantation of magnesium alloy AZ31 [8].

2.2.3 Polymers

Polymers are a diverse group of biomaterials consisting of long chain, organic molecules that have a wide range of uses, including surgical tools, implantable devices, device coatings, catheters, vascular grafts, injectable biomaterials, and therapeutics. Some examples of synthetic polymers include polyvinyl chloride (PVC), polyethylene (PE), polypropylene (PP), polymethylmethacrylate (PMMA), polystyrene (PS), polytetrafluoroethylene (PTFE), polyesters, polyamides (nylon), polyurethanes, polyetheretherketone (PEEK) and polysiloxanes (silicone). Natural polymers that are commonly used in biomedical applications include collagen, hyaluronic acid, heparin, and DNA. The use of polymers in the field of biomedicine has several advantages, including low cost, ease of manufacturing, a long history of use, and versatility. [9].

The impact of sterilization techniques on polymers is an important consideration in medical applications. There are several options for sterilizing polymers, but each method has the potential to cause instabilities or alter the properties of the material. Dry heat sterilization, which involves temperatures above 160 °C, can be effective, but it may be too high for certain polymers, causing them to degrade or melt. Steam sterilization, or autoclaving, occurs at lower temperatures, but certain polymer chemistries may react with the water vapor. Radiation treatment can also alter properties through crosslinking or bond cleavage. Chemical sterilization is a commonly used method that occurs at low energies and is generally inert with respect to most polymers. However, it is important to carefully consider the impact of sterilization techniques on the specific polymer being used to ensure its stability and performance in medical applications [1].

2.2.4 Composites

Composite materials are solid materials that consist of two or more distinct constituent materials or phases on a scale larger than the atomic level, resulting in significant changes in properties like elastic modulus compared to homogeneous materials [10].

In the field of biomaterials, ensuring the biocompatibility of each constituent in a composite is vital. Additionally, it is crucial that the interface between these constituents remains unaffected by the body's environment. Several applications of composites in biomaterials include dental filling composites, reinforced methyl methacrylate bone cement and ultra-high-molecular-weight polyethylene, as well as orthopedic implants with porous surfaces [10].

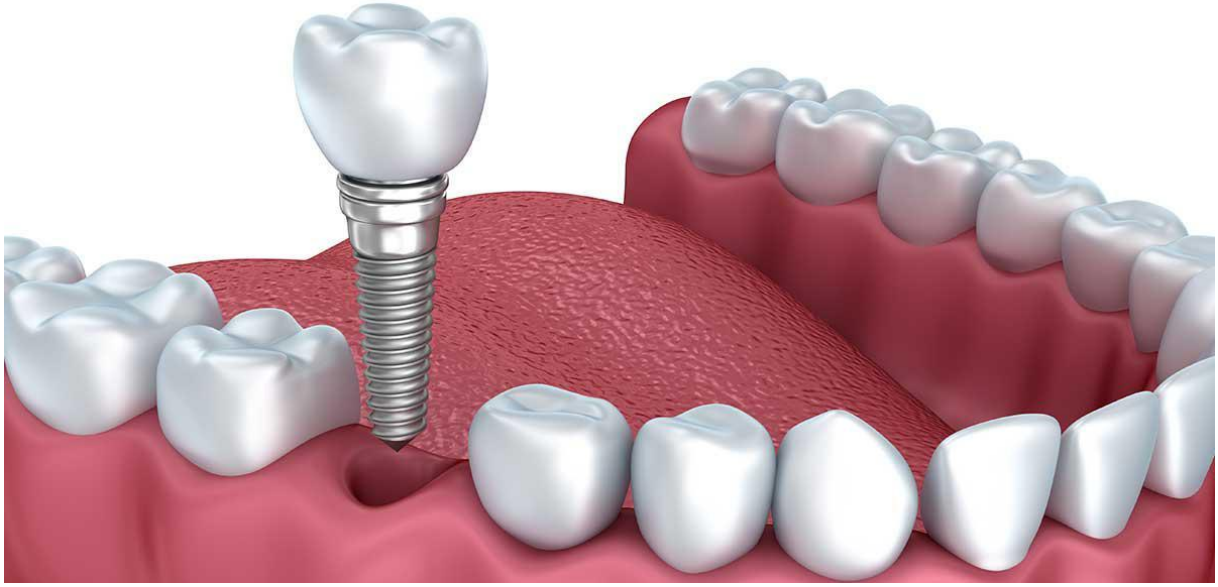

Figure 1: Titanium dental implant [52].

.

2.3 Hard tissue implants

Replacing or restoring bones presents several challenges, whether using endogenous (naturally produced or generated within an organism or system) or exogenous materials (originated from artificial sources and introduced into an organism or system from the outside). Endogenous substances are limited in quantity and may require an additional surgery, while exogenous implants can carry the risk of disease transmission or rejection by the body and are generally less biocompatible than endogenous materials. To address these issues, artificial materials used as bone replacement implants must closely mimic the structure and chemistry of natural human bone to be successful [2].

The types of hard tissue implants encompass various applications with specific considerations and requirements. For bone fixation, wires and screws made from bioresorbable materials are

preferred to avoid the need for additional surgeries. Magnesium alloys without aluminum content, such as Mg2Ag, show promise in this regard [11].

Dental implants aim to establish a strong connection with the jawbone, achieved by screwing a titanium stem (usually made from Ti6Al4V) into the bone and placing a ceramic crown on top [9].

Skull replacements should be lightweight, durable, and customized to accurately replicate the shape of the individual's head. Bioresorbable materials are often used for pediatric cases to accommodate growth and development [9].

In bone replacements, minimizing and preventing relative motion between the implant and surrounding tissues is crucial, which is accomplished by matching the elastic modulus of the implant to that of bone. This can be achieved by reducing the modulus through the material's chemical composition or by employing implant structures with specific designs, such as 3D-printed lightweight structures [9].

Joint articulation implants (Figure 2) require ensuring good mutual articulation, long lifespan, and minimal friction. This can be achieved by incorporating polymer inserts to reduce friction and ensuring a securely fitted stem that integrates well with the bone [12].

All these types of implants share one common need, which is a strong connection between a certain part of the implant and the surrounding bone. This can be challenging for bioinert materials, where there is no chemical bonding between the bone and the implant. Additionally, even inert materials undergo dissolution in the human body, which can lead to unwanted reactions to certain elements and complicate the healing process [1].

Therefore, there is a need to modify the implant surface. There are several options to achieve this. One approach is to structure the implant and increase its surface area, thus improving cell adhesion. This can be accomplished through techniques such as sandblasting by Al_2O_3 or TiO_2, where the grain size is crucial (smaller grains yield better results) [13].

Another method for surface structuring is etching in mineral acids such as HCl and H_2SO_4, which alters the surface morphology on a microscopic scale and enhances osteogenesis. Anodic oxidation is another possibility. Depending on the material, electrolyte, voltage, current density, and oxidation time, micro to nano pores are formed, which again improve cell adhesion and promote tissue integration [13].

A widely used option is coating the surface with a different bioactive material. Plasma spraying is commonly employed for this purpose, as it allows for easy application of calcium phosphates, which are bioactive and accelerate bone integration. However, it may not always achieve ideal adhesion and microstructure. Other methods include sol-gel, PVD, CVD, and more recently, cold spray, which can coat materials with low melting points that would not survive plasma spraying. For example, Daroonparvar et al. investigated titanium coatings on a magnesium AZ31

substrate using cold spray, where a Ti/Ta-coated magnesium was exposed to Hank's solution for seven days. The coating acted as a protective shield for the substrate, preventing any dissolution of the magnesium alloy [13].

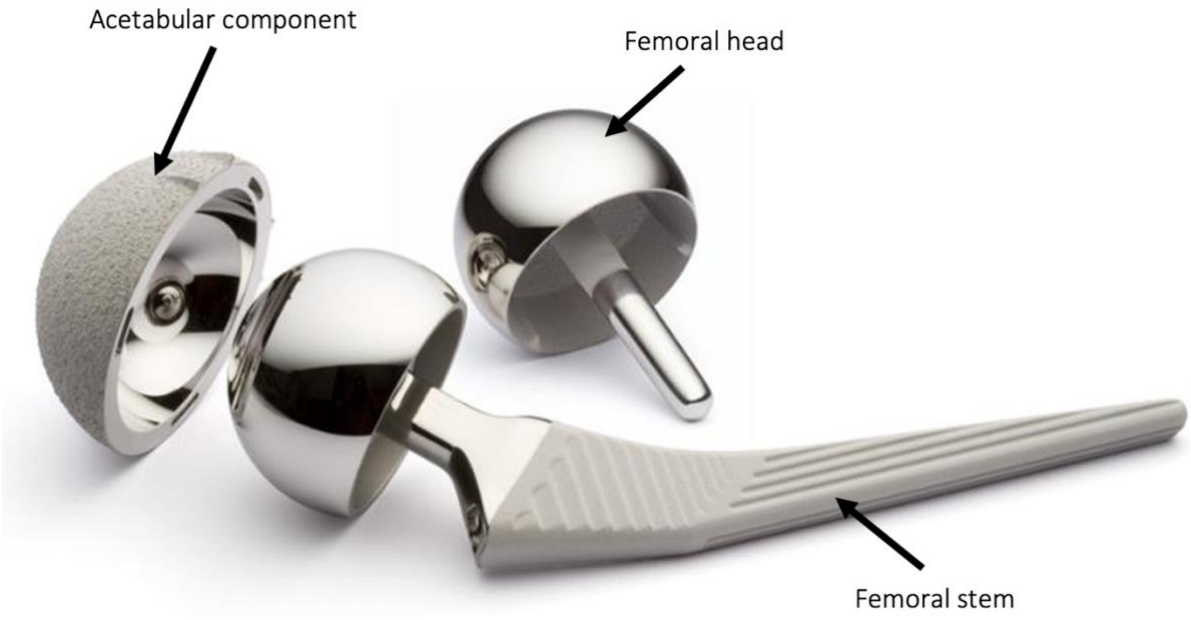

Figure 2: Hip replacement implant [11].

2.4 Cold spray

Cold spray technology is a solid-state coating process that utilizes plastic deformation of mostly metallic particles to adhere to a substrate and form a dense coating. It is an advanced manufacturing technique that has been developed over the past two decades and has found applications in a variety of fields, including aerospace, automotive, and biomedical [14].

The principle behind cold spray technology is based on the concept of kinetic spraying, which involves the acceleration of particles to high velocities through a supersonic gas jet. Powder particles are fed into a cold spray gun from a feeder, and a high-pressure gas source, like nitrogen, creates a supersonic jet that accelerates particles through a de Laval nozzle with velocities of up to 1200 m/s [10]. A typical cold spray gun is presented in Figure 3 [15].

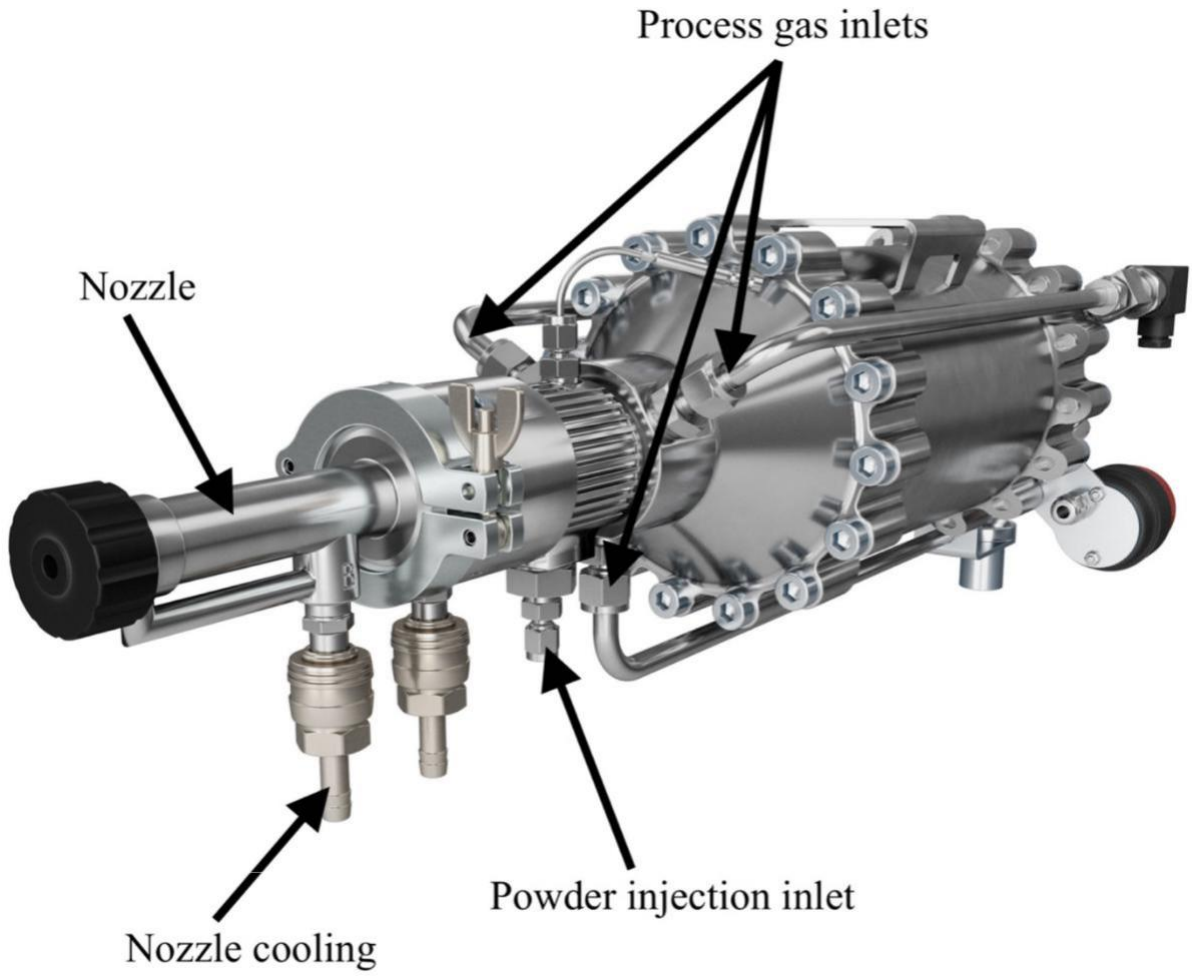

Figure 3: A cold spray gun by Impact Innovations [15].

2.4.1 Coating formation and structure

Before the cold spray process begins, the surface of the substrate must be properly prepared to ensure good adhesion of the coating material. The preparation involves cleaning the substrate to remove any dirt, oils, or other contaminants that may deteriorate the adhesion of the coating. The surface may also need to be roughened or profiled to increase the surface area for better bonding. This can be achieved through various methods, including grit blasting, acid etching, or mechanical abrasion. The choice of surface preparation method will depend on the substrate material, the coating material, and the desired end-use application [16].

During the deposition process, the initial layer of particles deforms the substrate's surface. As the first thin layer of particles is deposited, the dislocation density within the coating material increases, resulting in increased strength and hardness. Material jetting occurs, which is the driving force behind two out of the three known bonding mechanisms in cold spraying. Those involve metallurgical bonding, which is the diffusive bonding between the two metals in contact; mechanical interlocking, which involves the formation of localized extrusions of the coating material into the substrate (or vice versa), creating a mechanical trap; and mechanical intertwining, a mechanism similar to interlocking but with a higher degree of entanglement between the substrate and the coating [16].

The magnitude of deformation is influenced by various factors, including the interaction between the substrate and particles, where the most critical factor is the difference in hardness between the base material and the particles, as depicted in Figure 4, which illustrates that spraying materials with similar hardness is most suitable. When using a hard coating on a soft substrate, the particles undergo minimal deformation and tend to embed themselves into the base material. Conversely, using soft particles on a hard substrate results in significant particle deformation, but without establishing a mechanical bond with the substrate, thereby negatively affecting adhesion [17]. After the first layer is deposited, incoming particles bond with each other, thus the hardness difference is zero and velocity and temperature of the particles during flight are the key parameters of interest.

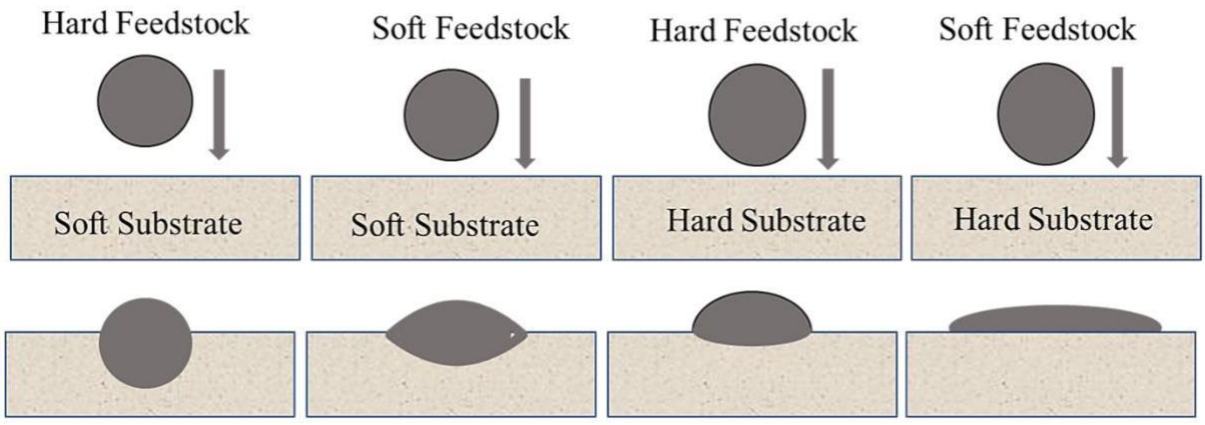

Figure 4: Particle-substrate interaction [17].

With each subsequent layer deposited, the particles undergo deformation and realignment through successive collisions, resulting in reduced porosity due to the hammering effect. The final cold sprayed coating ideally exhibits a dense and deformed structure, showcasing excellent adhesion and minimal porosity.

One of the prerequisites for creating a high-quality coating is having particles of sufficient size, ideally 10-50 microns. When spraying smaller particles, a phenomenon called bow shock occurs, which hinders effective deposition. Bow shock is caused by the abrupt deceleration and curvature of the gas stream in the vicinity of the substrate, creating a stagnant zone at the interface between particles and the substrate that impedes the movement of incoming particles. This results in a drop in the particles' velocity under its critical value, making it impossible for particles to deform and form a coating [2].

During the impact, the particles experience high deformation and strain rates, leading to the formation of shear bands. These bands are narrow regions of localized plastic deformation that can lead to adiabatic shear instability. This phenomenon occurs when the material is subjected to high strain rates, causing the dissipated energy to increase the temperature and soften the material. As a result, the rate of strain hardening decreases, and the flow stress reaches a maximum value, beyond which the flow stress reduces monotonically with plastic strain. The softening can persist indefinitely in an ideal material, but in real materials, fluctuations in stress, strain, temperature, or microstructure, and the inherent instability of strain softening can cause plastic flow localization. Shearing and heating become highly concentrated, while the straining and heating in the surrounding regions come to a halt, causing the flow stress to rapidly drop to zero. This process can be visualized using simple schematics, as shown in Figure 5 [18].

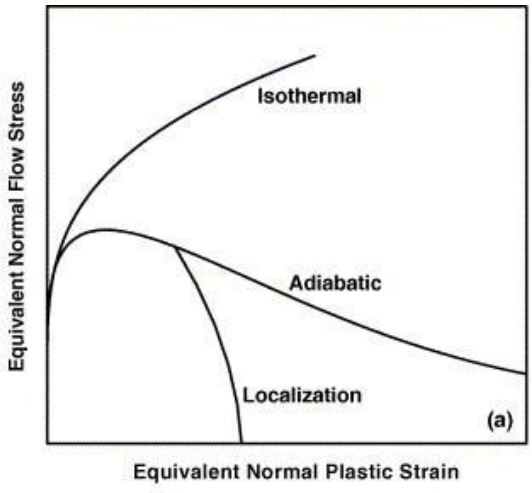

Figure 5: : Stress-strain curves for work-hardening materials (isothermal), adiabatically softened material (Adiabatic) and for materials under adiabatic shear localization (Localization) [18].

The literature is rather conflicted about the consequences of this effect. A paper by A. Joshi suggests that adiabatic shear is the cause of material jetting, one of the cold spray bonding mechanisms and therefore is required for coating deposition [19]. However, recent studies showcase that thermal softening is not necessary for cold spray deposition at all [20]. Instead, they suggest that pressure release is the origin of jetting in microparticle impact. Raising the impact velocity leads to elevated pressures caused by the impact, consequently resulting in increased reflected tensions. When the hydrodynamic tension during this transient phase surpasses the dynamic strength of the material, spall (fragmentation of a material) occurs. This phenomenon manifests as an unsteady ejection of material in the form of a jet and microscopic fragments [20].

2.4.2 Process parameters

The parameters of the cold spray process and the resulting coating formation are interconnected. The kinetic energy of the particles, which is influenced by factors such as gas temperature and pressure, the type of propellant gas, nozzle design, and particle size and shape, provides the work necessary for viscoplastic deformation. Most of this energy dissipates as heat upon impact, while a minor portion, approximately less than 10%, is retained as elastic energy associated with material imperfections or residual stress [21].

For a material to be successfully coated using the cold spray process, it must be sprayed at a velocity within a certain range known as the window of deposition. This range is defined by the critical velocity, or the minimum velocity needed for material jetting to occur, and the upper limit, beyond which materials lose their ability to attach to the substrate and cause erosion instead. If the velocity is too low, particles will only have an abrasive effect on the surface of the substrate and will be unable to form a coating. Equation 1, provided by Schmidt et al. [22], can be used to estimate the critical velocity for a typical 25-µm diameter particle.

$$v_{cr} = \sqrt{\frac{A\sigma}{\rho} + Bc_p(T_m - T)}\,, \qquad \text{(Eq.1)}$$

Where ρ is the density of the material, σ represents the flow stress of the material being sprayed, c_p is the heat capacity of the material, T_m is the melting temperature of the material, T is the average in-flight temperature of the particles and A and B are fitting constants [22].

2.4.3 Types of cold spray

Cold spray systems come in different configurations, mainly differing in their attainable chamber pressure and thus range of sprayable materials.

High pressure cold spray

High pressure cold spray, characterized by gas pressures typically ranging from 10 to 60 bar, involves the use of micron-sized particles and is commonly performed in an open air or near-atmospheric pressure environment. Powder is fed into the convergent part of the nozzle. This method of cold spraying is the most widely employed and is specifically the one used in our study [23].

Low pressure cold spray

The low-pressure cold spray system differs from its high-pressure counterpart primarily in terms of gas pressures, which are below 10 bar, and the powder entry point, which is in the divergent part of the nozzle. As a result, the achievable impact velocities in the low-pressure system are significantly lower. This method is considered a precursor to modern cold spraying techniques. Consequently, the scope of application for the low-pressure system is somewhat limited in comparison. One advantage of the low-pressure cold spray is its smaller size (the smallest one being the size of a suitcase), which makes transporting the system possible. [24].

Vacuum cold spray

Vacuum cold spray, alternatively referred to as aerosol deposition, represents a scaled-down version of cold spray that operates under partial vacuum conditions and utilizes submicron powders. It is predominantly employed in the application of ceramic coatings and has gained increasing attention, particularly in the realm of electronic device applications [25].

2.4.4 Input powders

The properties of input powders are crucial to a successfully deposited cold sprayed layer.

Atomized powders

Powders produced by gas, ultrasound, plasma, or other means of atomization possess excellent flowability, which ensures smooth and consistent feeding during the cold spray process. With controlled particle sizes ranging typically from 15 to 60 microns, atomized powders exhibit good sphericity, promoting favorable flow characteristics and enhancing particle adhesion [26]. Additionally, their typical high purity and homogeneity improves the coating properties.

Ball milled powders

In cold spraying, ball milled powders are used due to their affordability and ease of production. These powders offer the advantage of easy mechanical alloying during the milling process [27]. It is also possible to produce milled powders with nanoparticle content or cermet powders, such as cobalt binder with tungsten particles [28]. However, the milling depletes the particles'

plasticity, resulting in very low deposition efficiency. They also typically have irregular shapes and poor flowability, making them overall inferior to atomized powders.

Aerosol

Aerosol input materials, although less commonly used, offer unique advantages in cold spraying, such as the use of brittle ceramics. They are composed of sub-micron particles with sizes ranging from 200 nm to 2 microns, dispersed into a carrier gas. The use of sub-micron aerosol particles allows for the deposition of fine coatings with improved surface finish and density [25].

2.4.5 Applications of cold spray

Cold spray has a wide range of applications in various industries mainly as a coating technique.

In automotive industry, cold spray has been used as a method of coating brake discs (Figure 7) made of cast iron in a metal matrix composite, which dramatically raised their wear resistance and consequently reduced brake dust emissions [29]. Another possible usage is coating the cylinder bores of an aluminum crankcase in a more wear resistant material to enhance its performance.

In electronic and semiconductor production, various materials like tantalum, niobium, titanium, silver, copper, and other pure substances can be cold sprayed on components utilized in the sputtering process. Sputtering targets are commonly employed to create coatings for semiconductors, glass, solar cells, and more. Tantalum sputtering targets are extensively used in the production of vital components found in modern electronics, such as microchips, memory chips, print heads, and flat panel displays. The ability of cold spray to form a coating of theoretical unlimited thickness also make it highly suitable for applying copper and silver coatings on surfaces such as electrodes and heatsinks [30].

Cold spray has also been successfully utilized to deposit biocompatible metallic materials such as titanium-based, iron-based, and cobalt-based alloys, as well as polymers like UHMWPE, HDPE, and PEEK, and certain ceramics including HA, HA-graphene, and TiO2 [30].

For fabricating metallic biomedical structures, cold spray offers a promising method that surpasses the strength of similar materials produced through traditional manufacturing processes. The small size and controlled porosity of these structures make them particularly well-suited for constructing biomedical components, such as replacement joints [31].

In addition to a coating technology, cold spray also offers the ability to repair broken components and owing to the unlimited thickness of a cold sprayed layer, the possibility of additive manufacturing.

Cold spray technology's unique solid-state deposition characteristic avoids defects caused by excessive heat input and high temperatures. It holds significant potential for repairing aerospace, naval, and automotive components. The U.S. Army Research Laboratory and the Department of Defense has invested substantial research funds into developing cold spray as a repair technique for damaged components like fighters, warships, tanks, and vehicles [32].

In terms of cold spray additive manufacturing (CSAM), NASA successfully developed a combustion chamber and rocket nozzle (Figure 6). Through hot fire testing, their lightweight components demonstrated promising results. In comparison to traditional electroplating methods, CSAM offers substantial advantages, including reduced lead time and improved efficiency [33].

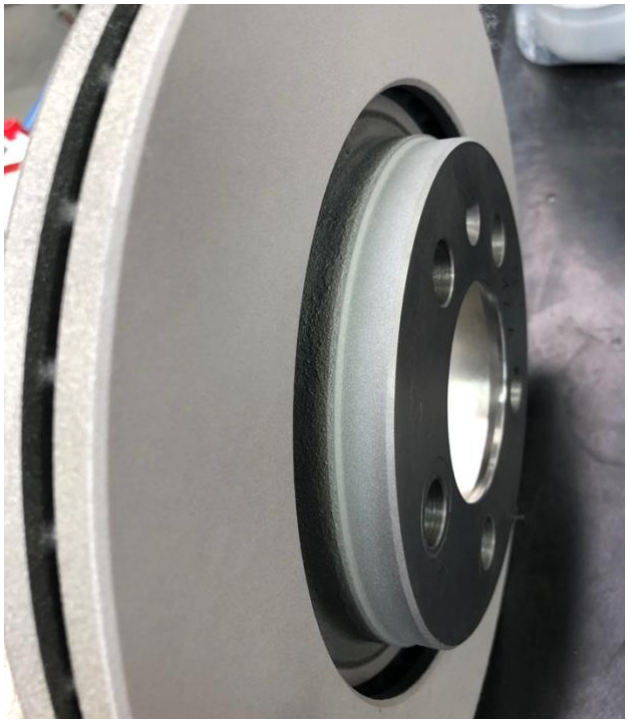

Figure 7: Cold spray coated brake disc [29].

Figure 6: NASA rocket engine manufactured by CSAM [33].

2.5 Plasma spraying

Plasma spray technology is a coating process that involves the use of a plasma jet to apply a coating material onto a substrate. The plasma jet is created by ionization of a gas, resulting in a plasma state where the gas forms a highly energetic stream. The coating material, which is typically in the form of powders, wires or suspensions is injected into the plasma jet and is melted and accelerated towards the substrate. Upon impact, the molten material forms a coating of a wide range of thicknesses (from tens to hundreds of microns) to complex-shaped components without the constraints of in-chamber processes, and at relatively lower costs than PVD/CVD processes [34].

2.5.1 Coating formation and structure

The structure of coatings formed by plasma spray methods is typically lamellar, resulting from the gradual deposition of numerous individual molten particles that solidify upon impact, gradually building up the coating as pictured in Figure 8. In addition to these lamellae (splats), the structure also consists of unmelted or partially melted particles, oxide inclusions, and pores. Oxide inclusions form in metallic coatings due to interactions between the molten particles and air, as well as heating of the coated surface during deposition. The concentration of oxide inclusions in the coating increases with higher temperatures and longer intervals between particle melting and impact on the surface. Excessive oxide content can reduce adhesion between individual splats and negatively affect coating properties, such as increasing brittleness. While oxide inclusions are generally undesirable, there are applications where they can be beneficial, enhancing wear resistance, hardness, and reducing thermal conductivity [35].

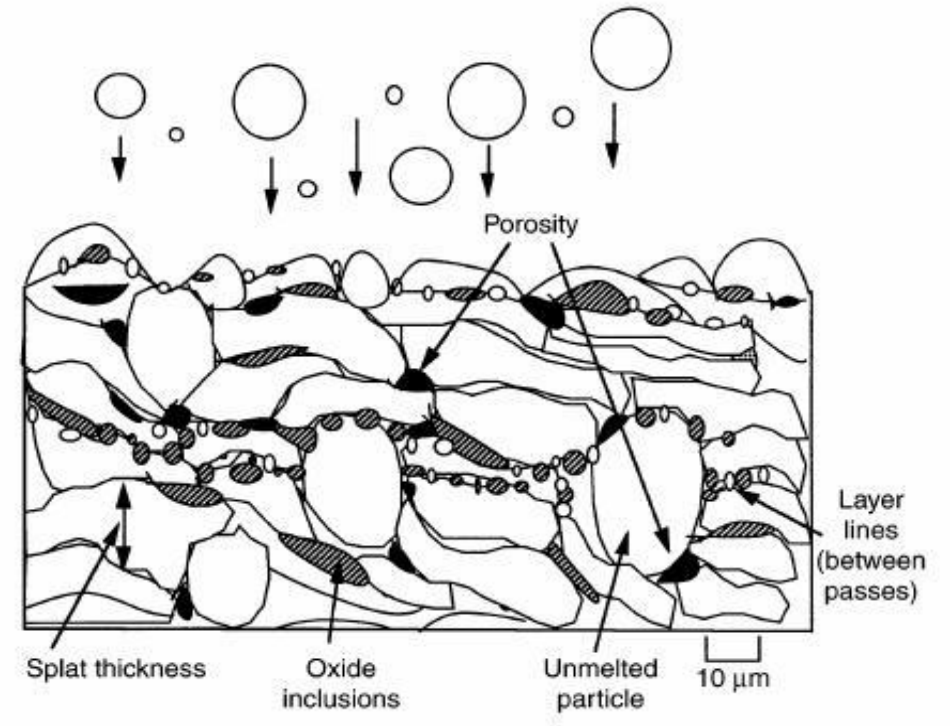

Figure 8: plasma sprayed coating structure [35].

2.5.2 Plasma generation

Plasma can be generated using various types of plasma torches. Consequently, each method differs in the plasma jet properties such as enthalpy, temperature and velocity.

DC plasma source

A DC arc plasma torch, the most widely used type among plasma torches, consists of a body containing a thoriated tungsten rod cathode and a water-cooled copper anode. The anode also serves as a nozzle to expel a high temperature plasma jet. Cold plasma-forming gas is injected into the torch body through an injection ring, which can create a straight or swirling gas injection (Figure 9). An electric arc is formed between the cathode and the anode, which ionizes the passing gas, creating a high velocity jet. The arc column is stabilized by the cooled anode wall and cold gas injection [36].

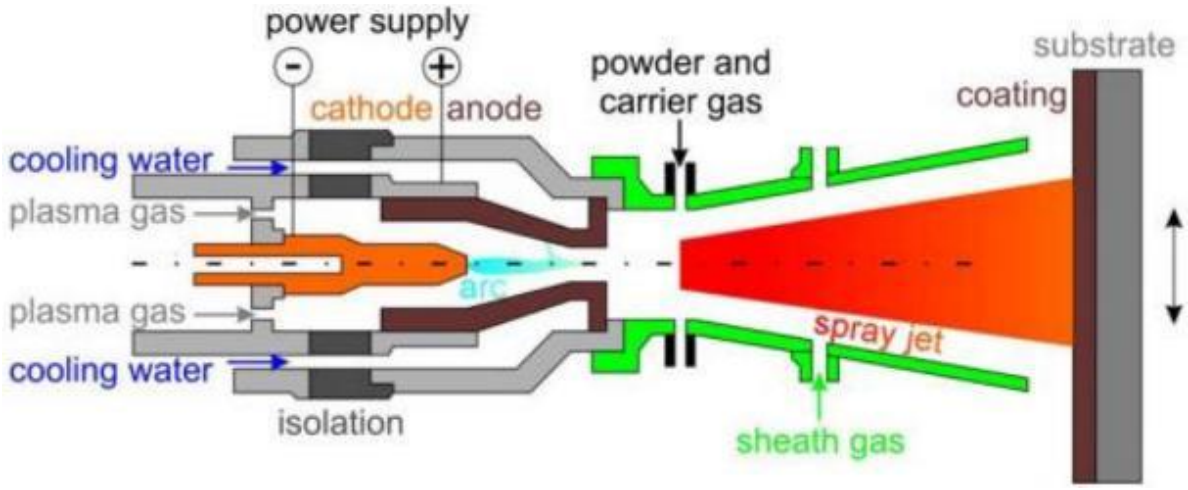

Figure 9: A typical DC plasma torch [57].

RF-ICP

Radio frequency inductively-coupled plasma technology (Figure 10) involves a gas flow (usually argon) through a nozzle inside a water-cooled copper coil. The nozzle is gas cooled and is typically made of quartz or other ceramics. The radio frequency generator creates an oscillating electromagnetic field which generates free electrons when the gas is ignited by a spark. The free electrons transfer kinetic energy to the gas atoms, heating them to the ionization temperature and creating an inductively coupled plasma. The plasma can reach temperatures of up to 10000 degrees Celsius, but is usually in the range of 5000 to 7000 degrees Celsius [35].

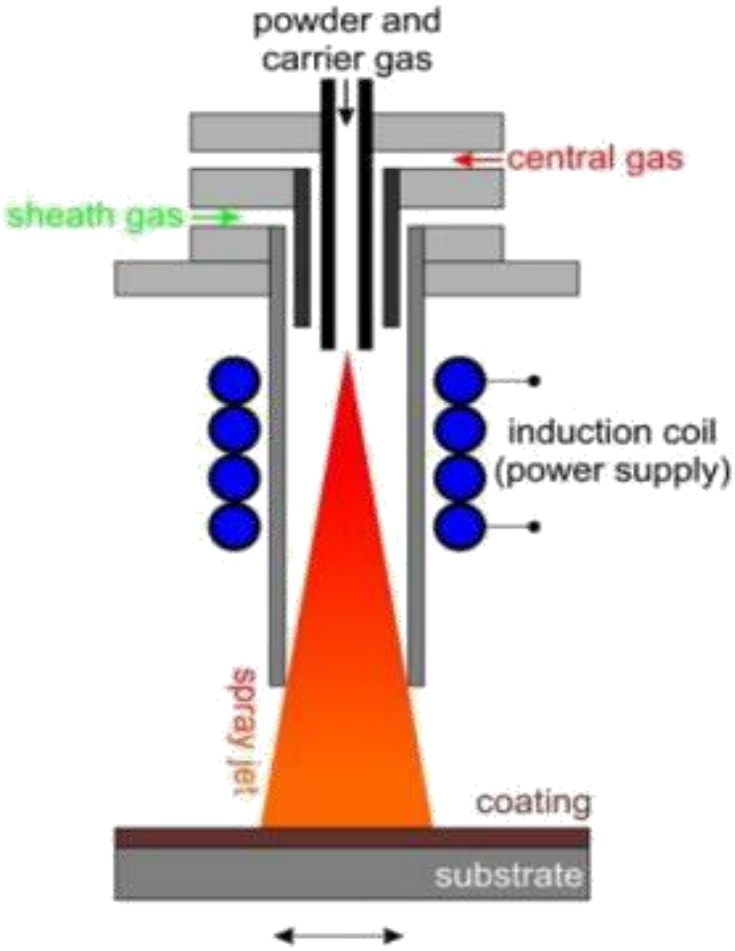

Figure 10: RF-ICP setup [57].

WSP

Water-stabilized plasma torches offer a viable alternative to traditional thermal plasma sources, such as DC arcs or RF discharges. By employing water walls, these torches can sustain relatively long arc columns with minimal gas mass flow rates through the torch chamber, resulting in high plasma temperature and enthalpy. These torches produce an oxygen-hydrogen plasma jet with exceptionally high flow velocities up to thousands of meters per second. This unique performance makes water-stabilized plasma torches ideal for demanding plasma spraying applications, such as the fabrication of dense, ceramic coatings [37].

WSP-H

Hybrid Water Stabilized Plasma Spraying is a new hybrid technology using a plasma torch that combines the advantages of a conventional DC gas-stabilized arc torch with those of a water-stabilized plasma torch. This torch design uses a combination of gas-liquid stabilization, where the plasma produced in an arc chamber with vortex gas stabilization flows into a second chamber and interacts with a vortex of liquid (see Figure 11). This setup allows for the control of plasma-jet characteristics across a broad range of parameters, extending from those typically seen in gas torches to those found in liquid torches. If argon is utilized for gas stabilization, the torch can maintain the thermal properties of a water torch, including high enthalpy and temperature, while substantially increasing the plasma density, velocity, and momentum flux [38].

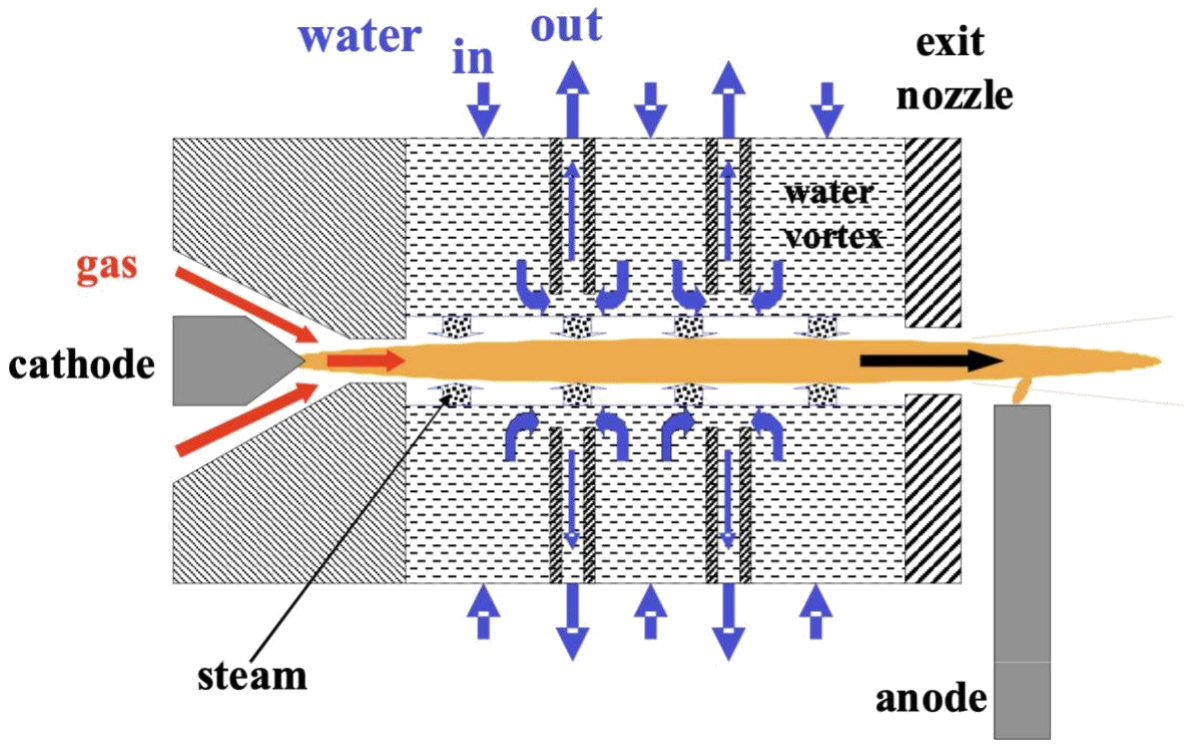

Figure 11: Hybrid gas/water plasma torch [58].

2.5.3 Environment

The environment in which the plasma spraying is performed is selected according to the reactivity of the sprayed material to atmospheric gases, mainly oxygen. If the material is not susceptible to oxidation, then atmospheric plasma spraying (APS) is the recommended, cost efficient method. However, if exposure to oxygen could have adverse effects on the quality of the coating, a controlled atmosphere is necessary. Controlled atmosphere plasma spraying (CAPS) is further categorized based on the specific type of protective environment employed.

Atmospheric plasma spraying

APS is a type of plasma spraying that is conducted at atmospheric pressure of around 100 kPa, making it a more versatile and accessible process compared to CAPS, because there is no need for vacuum or any controlled atmosphere. APS can be used with a variety of coating materials, including ceramics, polymers, and metals, although metallic powders are likely to oxidize during the process. One of the main advantages of APS is its ability to produce thick coatings quickly and efficiently, making it well-suited for applications where high deposition rates are required. However, APS coatings may have higher porosity and lower density compared to vacuum sprayed coatings, which can affect their mechanical properties. To overcome this limitation, additional measures such as the use of shrouding gas or multiple torches can be employed [39].

Inert plasma spraying

Similar to APS, inert plasma spraying (IPS) is also carried out at 100 kPa, but with the difference that a protective atmosphere is used. Either the entire system is positioned in a chamber filled with protective gas or the gas is blasted around the plasma stream, shielding it from the surrounding atmosphere while allowing the incident particles to solidify in the inert environment and avoid oxidation of the coating. This method enables reactive metals such as tungsten and copper to be sprayed [40].

Vacuum plasma spraying

Vacuum plasma spraying (VPS) is a type of plasma coating process that takes place in a controlled low-pressure atmosphere instead of atmospheric pressure, which minimizes the interaction between the plasma jet and the oxidation inducing environment. This has several benefits compared to the traditional APS process. For example, the VPS process reduces the oxidation of both the powder and the sprayed deposits, resulting in a more controlled and uniform coating microstructure with less contamination. Also, VPS produces a much longer plasma jet compared to APS, meaning the particles have more time to thoroughly melt. This makes it possible to successfully deposit reactive metallic materials such as tungsten, which can be challenging to coat using other methods due to both its high reactivity and high melting temperature. The VPS process has been found to produce coatings with lower porosity and better adhesion compared to APS coatings [41].

High pressure plasma spraying

In high-pressure plasma spraying (HPPS), increasing the pressure (up to 400 kPa) shortens the plasma plume, reducing the free path length of plasma elements. This results in increased arc resistance and input voltage, but also raises heat losses through water-cooled nozzles. However, it brings steeper temperature gradients, higher axial temperatures, and a concentrated energy density within the plasma. To prevent nozzle damage, a low hydrogen content plasma gas mixture is required, along with a high plasma-gas flow rate. HPPS coatings demonstrate improved density, hardness, and homogeneity due to higher pressures and plasma temperatures. This is particularly beneficial for ceramic coatings, as they exhibit minimal presence of unmelted particles [42].

Reactive plasma spraying

Reactive plasma spraying (RPS) offers a viable solution for the fabrication of, e.g., nitride ceramics and other challenging compositions that are difficult to deposit using traditional thermal spray methods. RPS uses a combination of a controlled nitrogen atmosphere paired with nitrogen carrier gas, which promote the plasma nitriding reaction of molten feedstock materials. The process relies on chemical reactions between elemental metal or non-metal powders and the atoms, ions, and radicals present in the plasma, to achieve the desired material compositions. Various nitride ceramic coatings, including titanium nitride (TiN),

aluminum nitride (AlN), iron nitride (Fe4N), and silicon nitride (Si3N4), have been successfully produced utilizing the RPS technique [43].

2.5.4 Input materials

Dry powders

Powders are the most common feedstock materials for plasma spraying. The initial morphology of the powder particles is a crucial factor in thermal spraying, as coatings made from powders with dissimilar particle morphologies can have significant structural differences, despite having the same chemical composition and particle size distribution. The morphology of feedstock powders governs its flowability as it flows through the feeder, pipeline, and the injection system. Poor powder flowability can cause several processing problems, including reduced efficiency due to repeated clogging of the feeder and injection system, fluctuations in powder feed rate leading to heterogeneities in the coating structure, and overheating and thermal degradation or detachment of existing coating layers. Powder flowability decreases as particle shape deviates from sphericity [44].

To achieve consistent heating and acceleration, plasma spraying commonly employs powders with particle sizes ranging from 10 to 90 µm in diameter. Powders with a narrow size distribution are typically preferred, as they help to ensure uniformity in the coating process. The two main types of powders utilized for plasma spraying are atomized and ball milled powders [44].

Suspensions

Suspension plasma spraying (SPS) is a modified thermal spray technique that allows for the creation of high strain-tolerant and low thermal conductivity coatings with porous, segmented, or columnar structures that resemble the microstructure of EB-PVD (electron beam physical vapor deposition) topcoats, but at a lower cost. This technique utilizes liquid feedstock containing submicron or nanometer-sized particles, which are suspended in water or ethanol-based solvents. Dispersants are added to the suspension to prevent the particles from agglomerating.

The SPS process involves several stages, including atomization of the suspension when it first contacts the plasma, followed by evaporation of the liquid carrier medium from the droplets once the solvent reaches its boiling temperature. As the liquid carrier evaporates, the fine particles in the suspension are exposed to even higher temperatures, which causes them to partially melt and form a liquid phase. Finally, as the particles move further within the plasma flame, they come into contact with the substrate and rapidly solidify, resulting in the deposition of a layer of material onto the substrate. Numerical studies have found that increasing the mass flow rate of the suspension and the torch power can enhance the deposition efficiency of the SPS process [45].

One of the key materials that has been sprayed using suspension plasma spray technology in biomedical engineering is hydroxylapatite. Obtaining ready-to-spray HA powder involves time- and cost-consuming processes such as atomization, calcination, and sieving, which can introduce impurities and deviate from the original phase composition. These processes also have a low yield, making them inefficient. Using HA solutions or suspensions for direct feeding into plasma torches is a simpler and more efficient method that can also create novel microstructures [46].

2.5.5 Applications of plasma spray

Plasma spraying has a wide range of applications across various industries. One of its main purposes is to provide protective coatings against wear and corrosion or to enhance functional properties in different components.

In the aerospace sector, plasma sprayed coatings are used to protect seal ring grooves in aero-engine turbines from fretting wear, utilizing materials like tungsten carbide/cobalt. Thermal barrier coatings (TBCs) based on zirconia are applied to turbine combustion chambers to enhance their heat resistance. In mechanical engineering, aluminum and chromium oxide. coatings are used on printing rolls to ensure wear resistance during laser and diamond engraving. Plasma spraying also finds its place in the automotive industry, where molybdenum alloys are sprayed onto diesel engine piston rings to improve their durability. Additionally, biocompatible coatings of hydroxyapatite are applied to medical and dental implants, making plasma spraying a valuable technique in the biomedical field [47].

2.6 Comparison

Cold spray and thermal spray methods differ in their energy input. Cold spray uses heat only to accelerate the particles through a nozzle, which remain solid, while thermal spray requires more energy to heat the particles beyond their melting point. This leads to phase transformation and often causes degradation of the coatings' mechanical properties due to oxidation and tensile stress formation. Vacuum plasma spraying can eliminate these issues, but it is more resource-intensive than cold spray. The diagram in Figure 12 shows the differences between the individual thermal spray technologies in terms of the in-flight particle velocity and temperature, and Figure 13 displays the differences in coating microstructure [48].

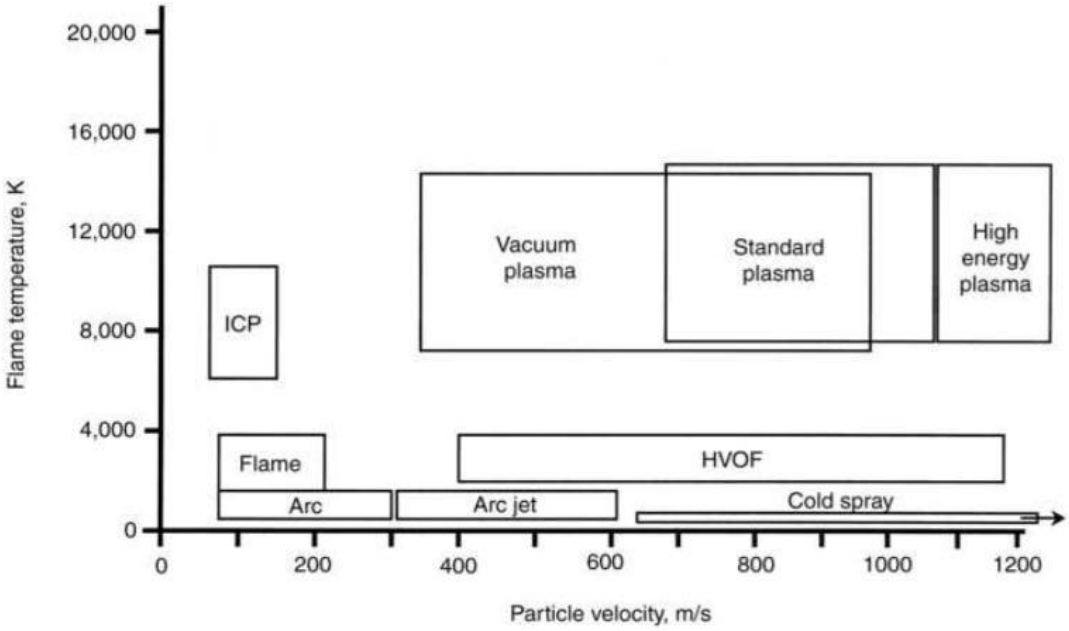

Figure 12: Particle in-flight velocity and temperature of different thermal spray methods [53].

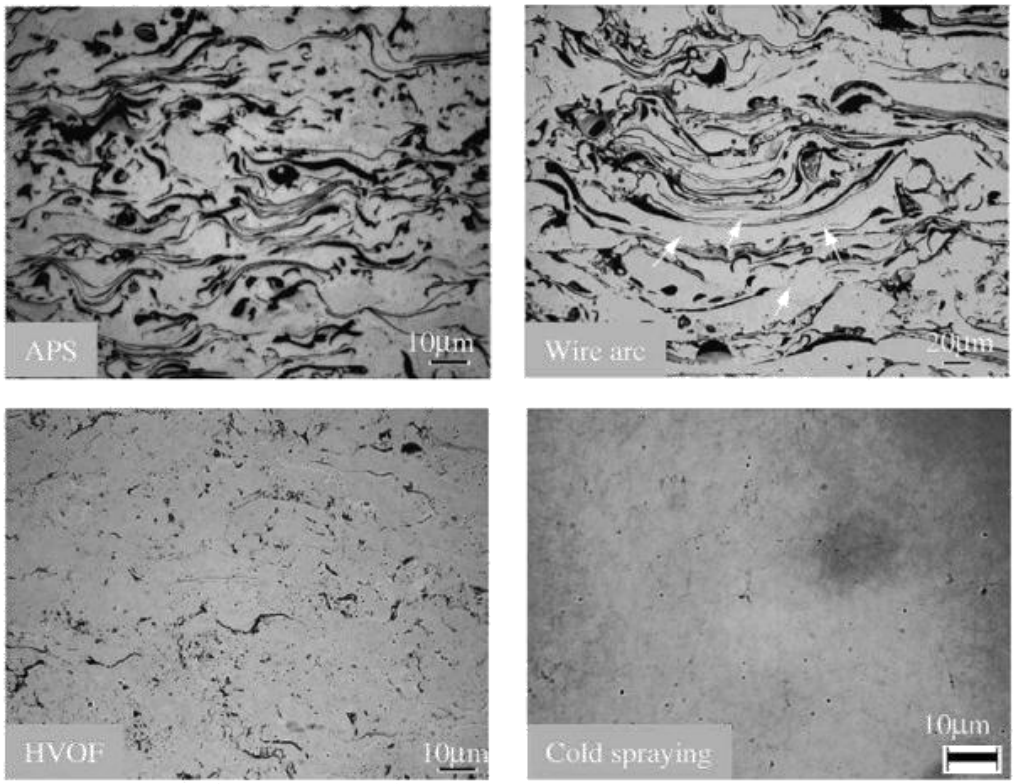

Figure 13: Coating microstructure of different thermal spray methods (illustrated using Ni-5 wt.% Al) [51].

Thermal spray methods have a wide range of material options due to the high temperatures used, but cannot be used for materials that have a low melting and evaporation temperatures. Cold spray, on the other hand, has a narrower range of sprayable materials that are mostly limited to those that can plastically deform, but it produces high purity, strong, and dense coatings, while also having higher efficiency and deposition rate [41].

By depositing a plasma sprayed porous bioactive hydroxyapatite (HA) coating on top of a dense cold sprayed titanium shielding coating on a magnesium alloy substrate, we aim to address the presented limitations by combining the advantages of each process. This hybrid coating strategy is mainly suited for areas where the implant interfaces with the natural bone, such as the shank of a hip replacement implant. The cold sprayed titanium serves as a thermal shield, protecting the reactive magnesium alloy substrate during plasma spray deposition, and, at the same time, acts as a chemical barrier against the corrosive environment of the human body. The HA coating, resembling human bone in its chemical composition, serves as an interface between the implant and the surrounding tissue, promoting bone cell growth and significantly accelerating the healing process. This innovative hybrid Cold spray/WSP-H coating onto a magnesium substrate holds promise for improving the success rate of hard tissue replacement surgeries.

3 Experimental

This section describes the input materials and the process of applying a hybrid cold spray/WSP-H coating onto a magnesium AZ31 substrate. The substrate was first coated with cold sprayed pure titanium and subsequently, a thermally sprayed hydroxylapatite layer was deposited on top using the WSP-H method.

3.1 Used materials

3.1.1 Titanium powder

We used a pure titanium powder provided by AP&C, a supplier based in Boisbriand, Canada, that holds ISO 13485 certification. X-ray diffraction (XRD) analysis (Figure 14) confirmed that the powder was composed entirely of a Ti alpha phase, with an average crystallite size of 191 nm. The average particle size was 15–45 µm, which is a smaller range than what is typically used in high-temperature thermal spray processes, but it is well-suited for a high-pressure cold spray process. The powder's regular, spherical morphology (shown in Figure 15) is a result of its gas atomization production technology, and this spherical particle morphology makes it ideal for cold spraying.

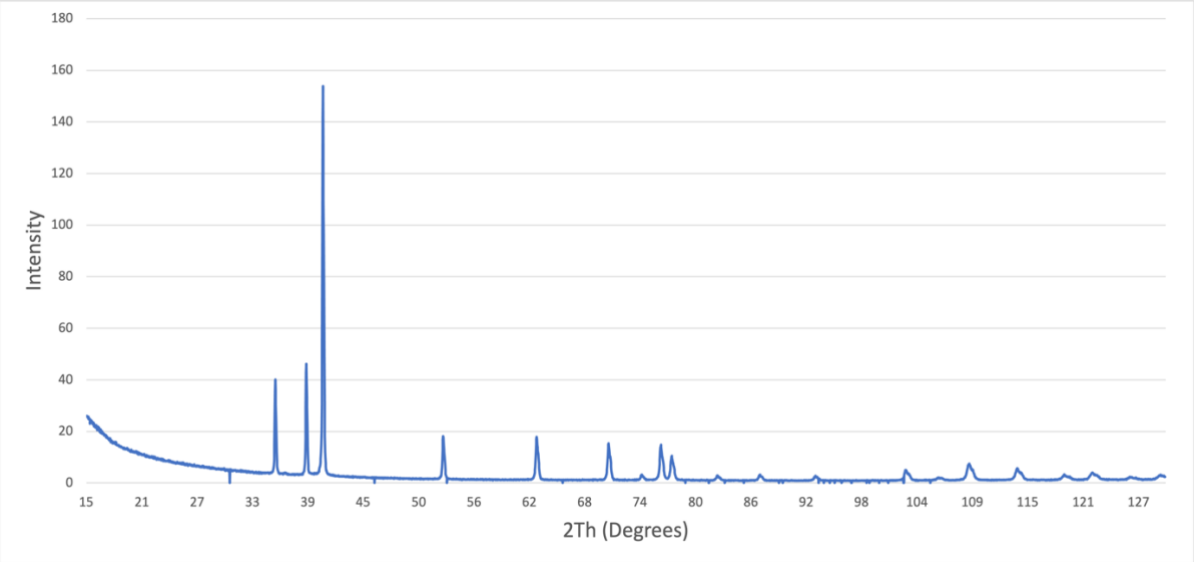

Figure 14: XRD analysis of the feedstock Ti powder. All visible peaks pertain to titanium alpha phase.

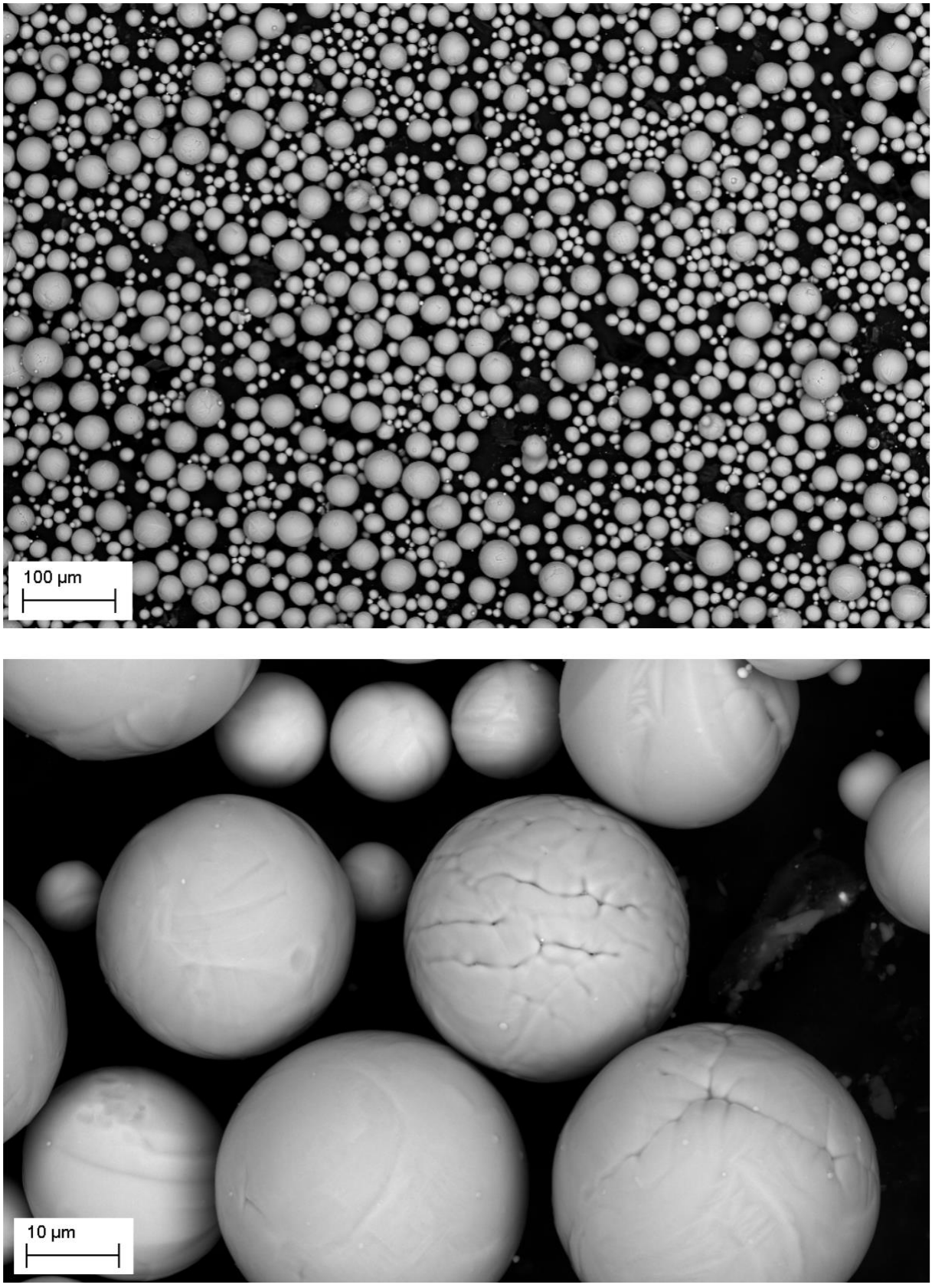

Figure 15: Ti feedstock powder particle morphology.

3.1.2 Hydroxylapatite suspension

The HA suspension was synthesized using a wet chemical process. In this process, $Ca(OH)_2$ was slowly added to H_3PO_4 at a temperature of 36.8 °C, which led to a neutralization reaction resulting in an aqueous suspension of HA. During the synthesis, the suspension was continuously stirred, and the reaction was halted once the pH reached approximately 9.0 [46].

To obtain a pure HA suspension, the aqueous suspension was allowed to settle for 48 hours to separate the excess water and the HA precipitate. The excess water was then removed, and fresh deionized water was mixed with the remaining HA suspension [46].

To assess the purity of the final HA suspension, a dried sample was subjected to XRD analysis, as shown in Figure 16. The analysis revealed that the HA phase was 100% pure and amorphous, with consideration of the detection limits of the machine. The morphology of the HA nanoparticles was observed using SEM and is shown in Figure 17. The nanoparticles crystalized in the form of small needle shapes 80 nm in length and 20 nm in width. The produced suspension also displayed a relatively high viscosity of 23 mPa·s at 20 °C (measured using a Brookfield DV2TLV viscometer), which is significantly higher than that of ethanol (1.082 mPa·s) or water (0.890 mPa·s). As such, the viscosity of the suspension was reduced by approximately 50 % by diluting it with deionized water to prevent clogging in the feed nozzle during the spray process [46].

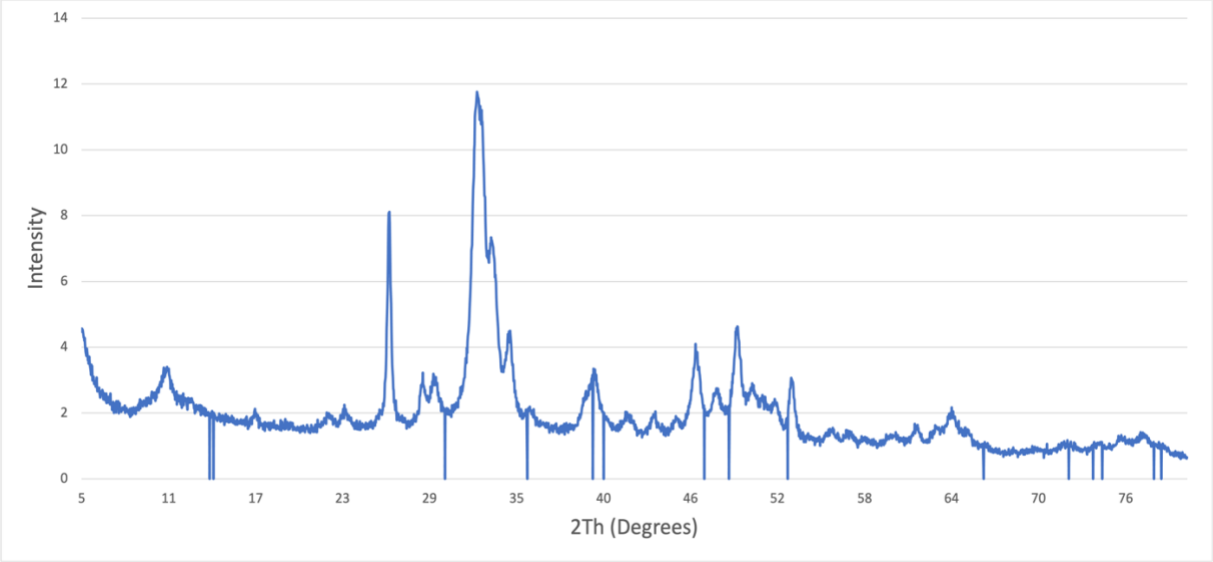

Figure 16: XRD analysis of the HA suspension [46]. All visible peaks pertain to hydroxylapatite phase.

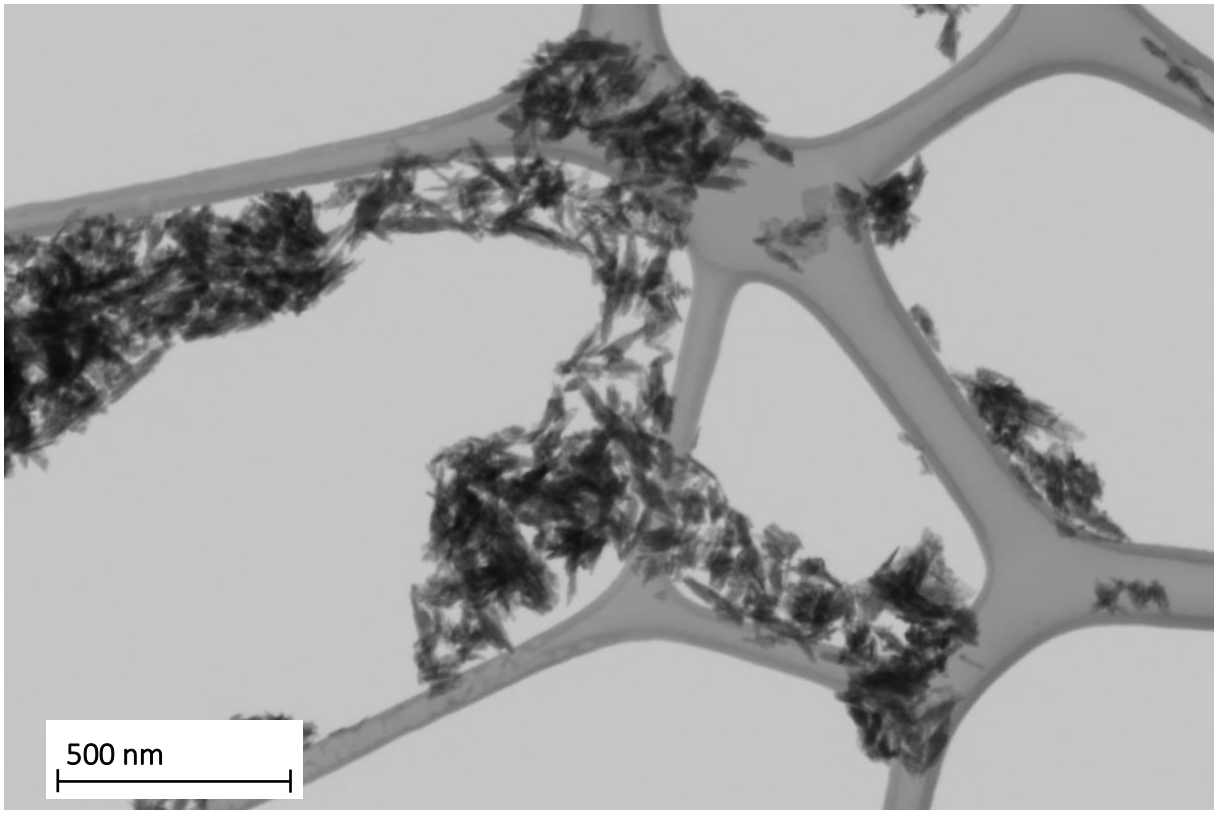

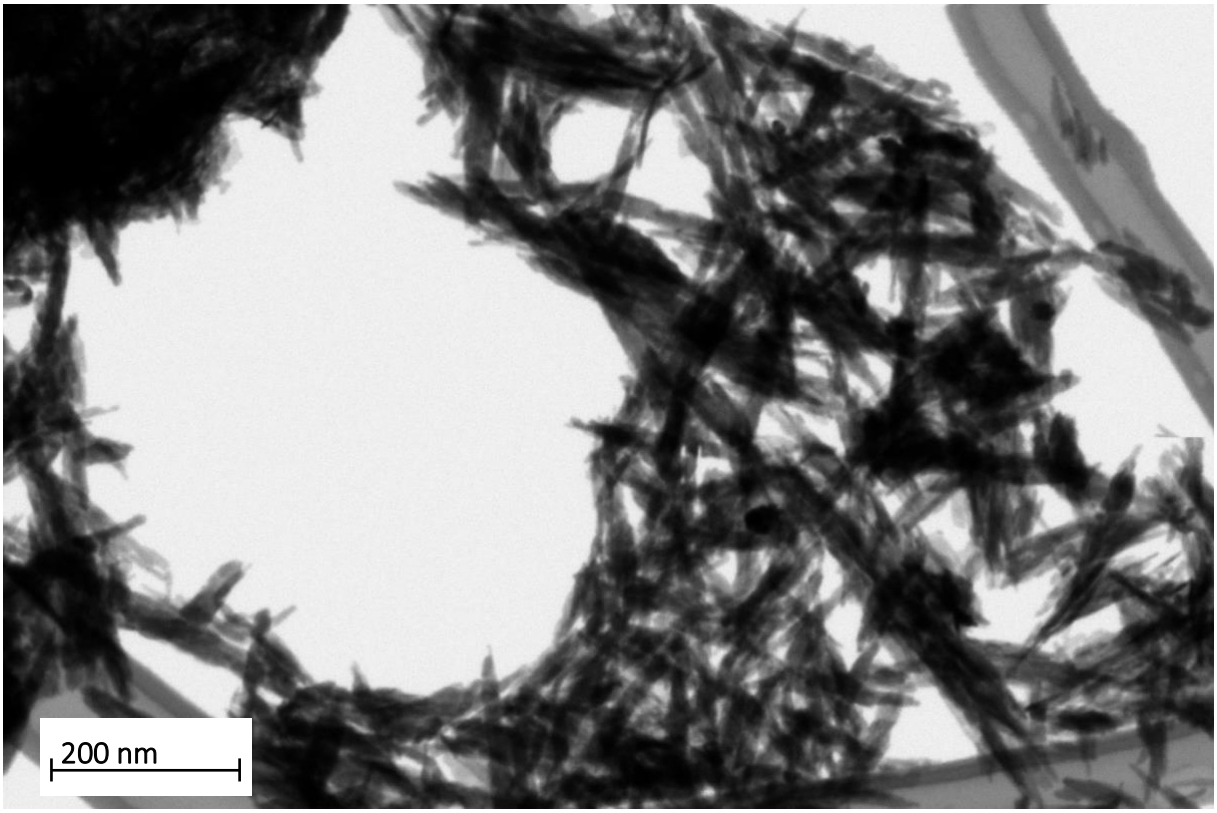

Figure 17: HA feedstock particles morphology.

3.1.3 Substrate

The substrate of choice was a cold-rolled and annealed AZ31 Mg-alloy, supplied by Alfa Aesar, GmbH. (Germany). Prior to deposition, the surface of the sample was grit blasted with spherical glass particles with typical sizes of 200-300 µm. This was followed by ultrasonic cleaning, realized in ethanol to prevent excessive oxidation.

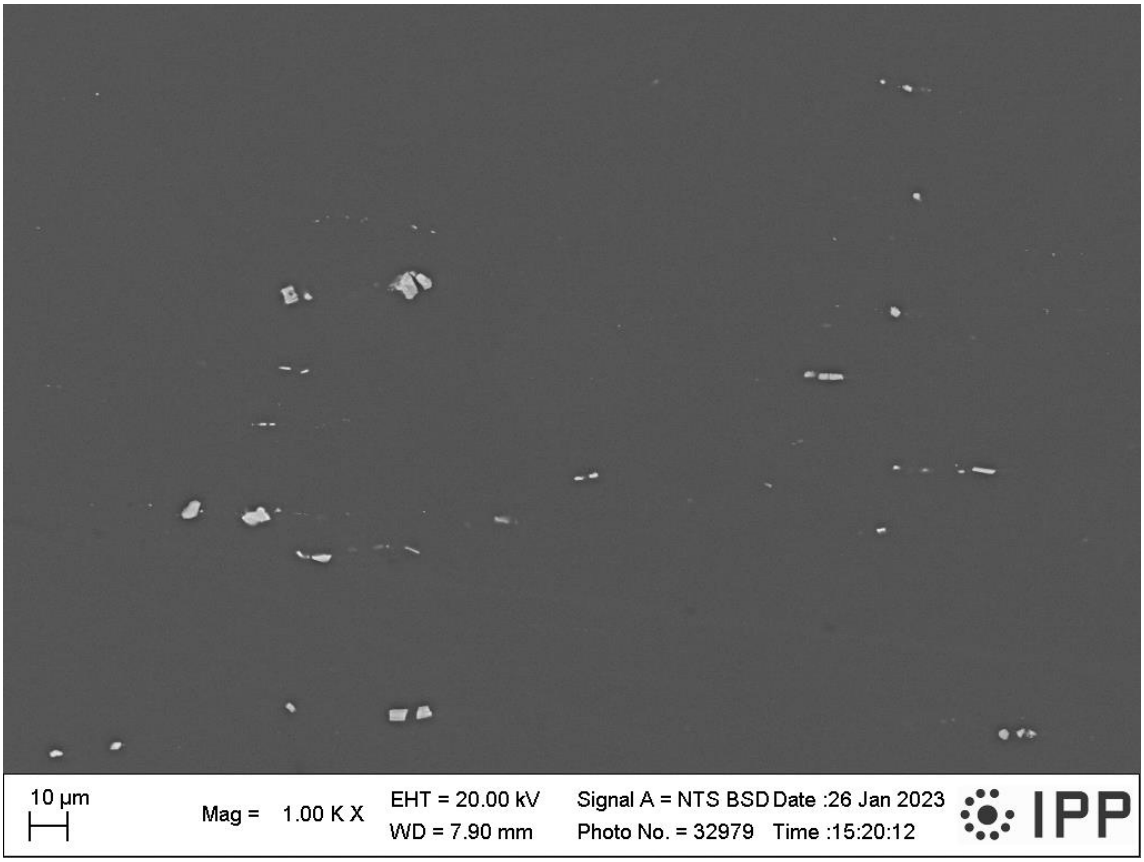

Figure 18: AZ31 substrate microstructure.

Table 1: AZ31 substrate chemical composition.

Element	Measured (wt. %)	Nominal (wt. %)
Mg	95.4	93.8–96.2
Al	2.7	2.5–3.5
Mn	0.2	0.2–1.0
Zn	1.3	0.7–1.3
0	0.4	0.4

Chemical analysis of the substrate was determined using EDX (Figure 18,
Table 1). The chemical composition we measured matches the nominal composition of an AZ31 alloy. The SEM image displays a homogenous matrix with uniformly dispersed aluminum precipitates. As the plasma spray process puts the materials under extreme thermal loading in the spray process, another, well-proven substrate was used for the HA deposition and later served as a control group. For this, samples of identical dimensions were prepared Ti6Al4V alloy (Grade 23 purity) and placed onto the carousel holder along with the Ti-sprayed AZ31 substrates. The two substrate types were then sprayed with HA in an identical run.

3.2 Coating deposition process

3.2.1 Cold spraying

Cold spray coating of Ti onto the AZ31 substrate was conducted in our partner laboratory at Politecnico di Milano in Italy, using a high-pressure cold spray system 5/8 from Impact Innovations GmbH (Figure 19). The system maximum limits are 50 bar gas pressure and 800 °C gas temperature.

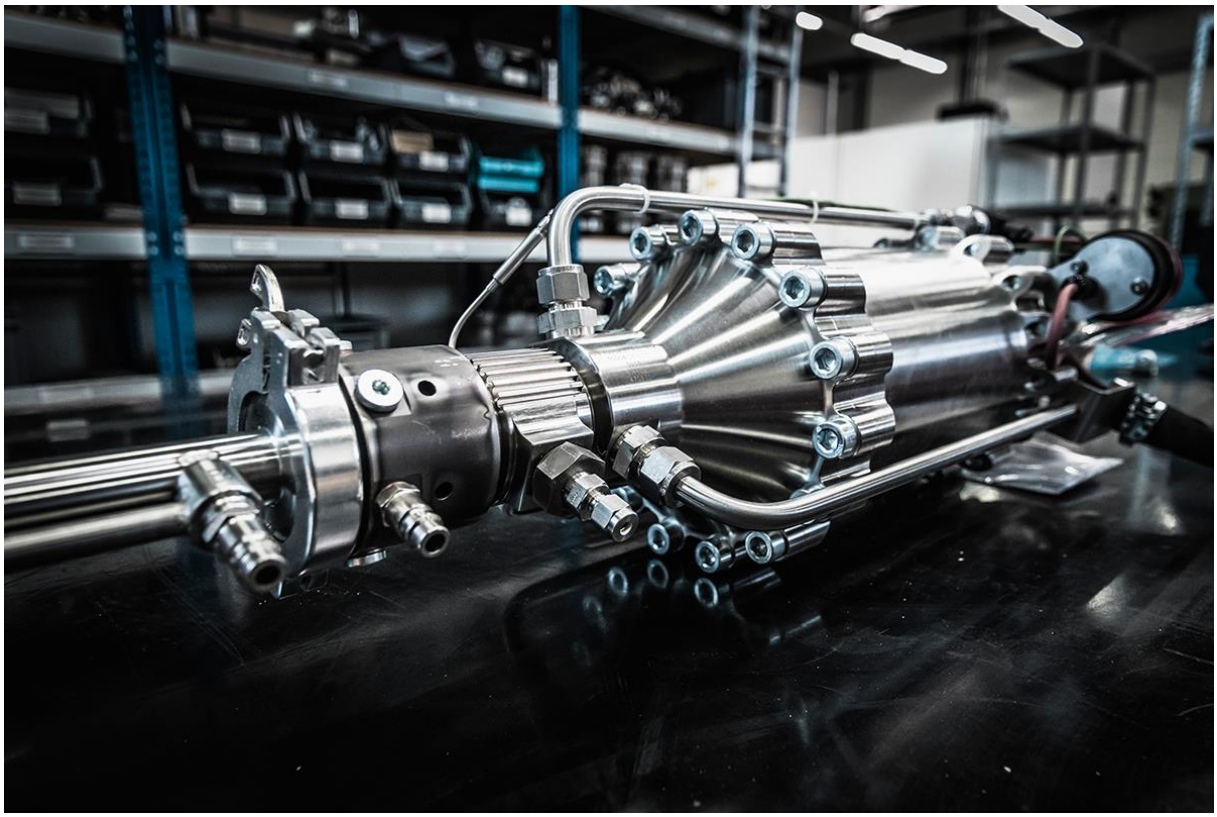

Figure 19: Cold spray 5/8 system at Politecnico di Milano. Image courtesy of Impact Innovations [15].

Nitrogen was used as the main process gas. The deposition conditions were set to the gas pressure and temperature of 45 bar and 700 °C, respectively. To prevent the reduction of particles' in-flight velocity caused by atmospheric interaction, a short stand-off distance of 25 mm was used, which is a typical distance used in cold spraying. The used deposition parameters can be found in Table 2.

Table 2: Cold spray deposition parameters for Ti coating on AZ31 substrate.

Deposition parameters	
Gas temperature (°C)	700
Work and carrier gas	Nitrogen
Gas pressure (bar)	45
Stand-off distance (mm)	25
Powder feed rate (g/min)	25
Torch traversal speed (mm/s)	300
Passes	4

3.2.2 WSP-H spraying

Hydroxylapatite coating was performed using the WSP-H 500 system at the Institute of Plasma Physics of the Czech Academy of Sciences (Figure 20). The hybrid WSP plasma torch has an adjustable power range of 100 to 180 kW. In comparison to other plasma torches with high energy, the Hybrid WSP produces plasma enthalpy that is one order of magnitude higher. This feature, along with the high power and temperature of the torch, makes it an excellent choice for efficient and cost-effective spraying of high melting point ceramic materials such as Cr_2O_3 and YSZ. Aside from dry powders, owing to the extreme net power of the torch, suspensions, and solutions can be well sprayed, as illustrated in Figure 21 [49].

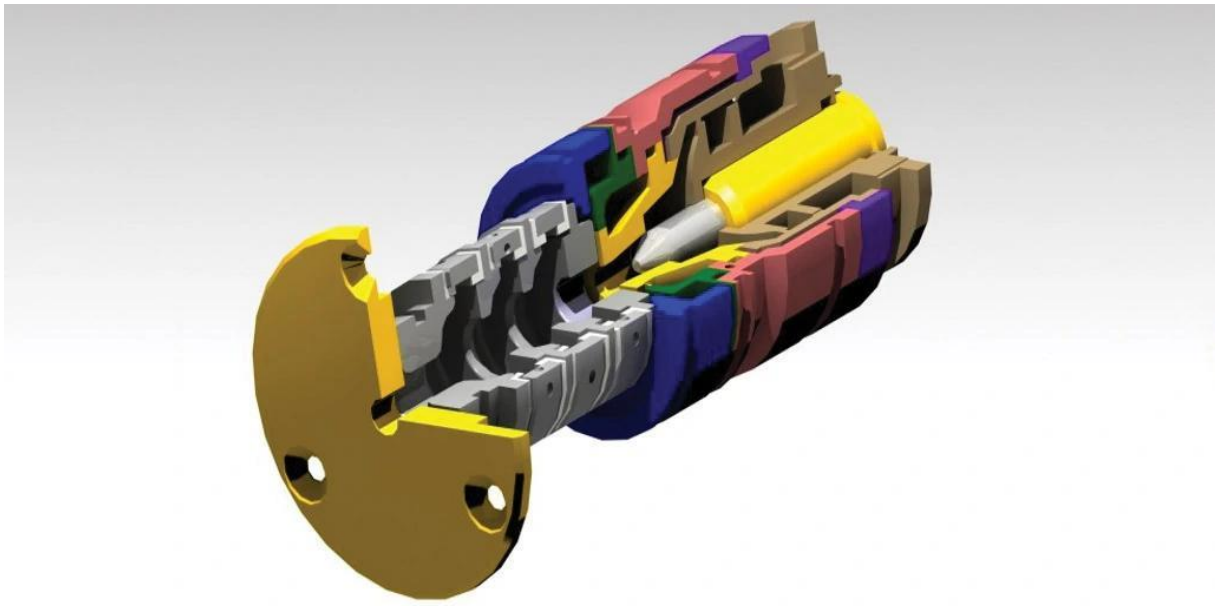

Figure 20: WSP-H gun anatomy [49].

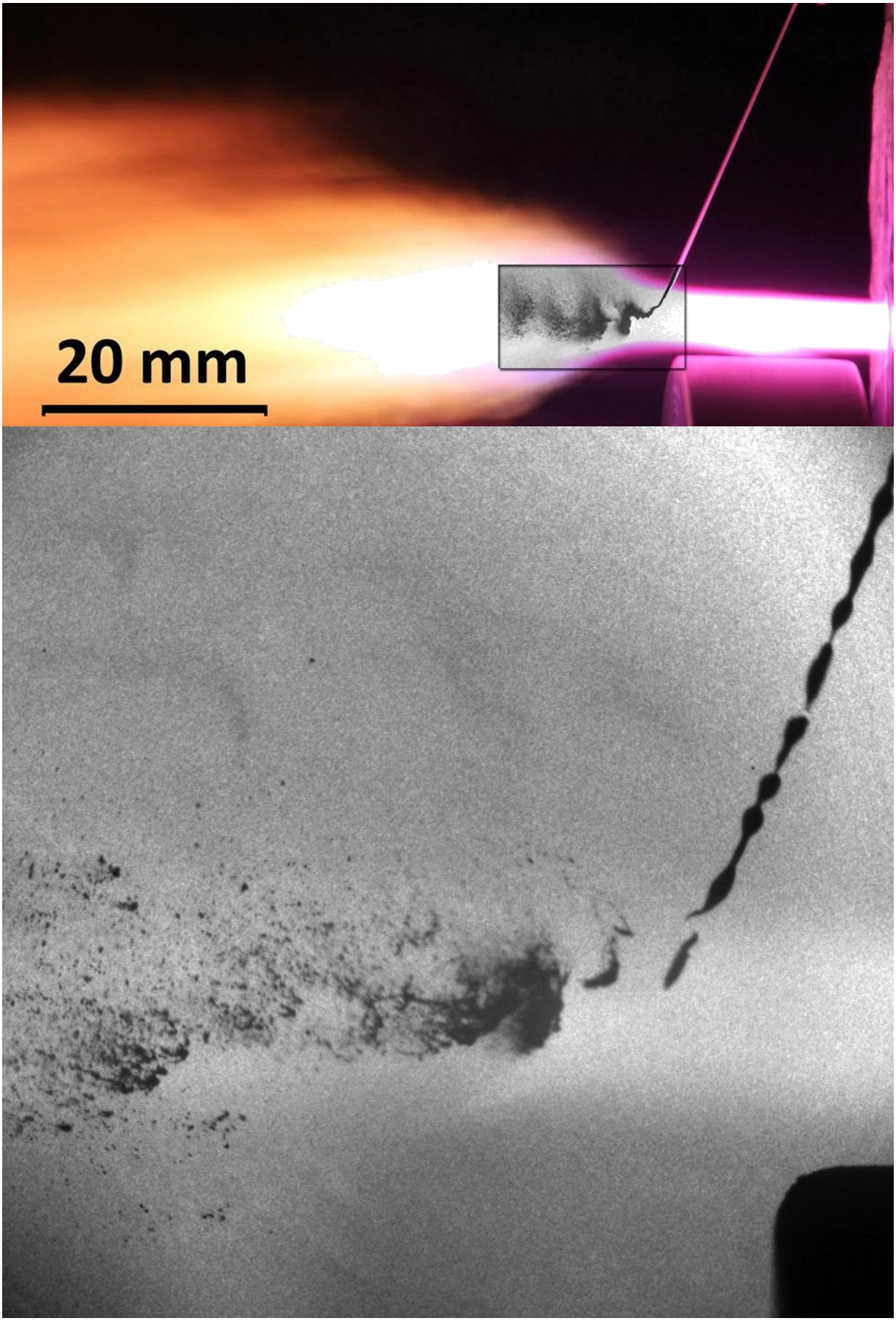

Figure 21: Suspension plasma spraying process [49].

The torch was operated at 500 A and generated a net power output of 150 kW. The suspension was injected into the plasma jet radially. To ensure optimal penetration of the suspension and facilitate proper evaporation of the liquid carrier as well as uniform melting of the deposited material, it was crucial to employ small-diameter feeding nozzles with minimal suspension divergence. Nonetheless, overly small nozzle diameters presented a risk of clogging, particularly during runs with a high number of torch passes, as encountered in this study. Consequently, a 0.35 mm sapphire nozzle was selected as a viable compromise feeding solution. Table 3 lists the spraying parameters used.

Table 3: WSP-H spraying parameters.

Deposition parameters	
Torch current (A)	500
Argon flow (slpm)	15
Feed angle (degrees)	20
Feed distance (mm)	20
Feed pressure (bar)	3.0
Stand-off distance (mm)	100
Powder feed rate (g/min)	97
Torch passes	312

3.3 Specimen preparation and characterization

3.3.1 Scanning electron microscopy

The coated samples were subjected to metallographic preparation for scanning electron microscopy (SEM) and energy-dispersive X-ray spectroscopy (EDX) analyses. This required preparation of metallographic cross-sections, a process that involved initial sectioning using a Struers Secotom-50 metallographic saw, fitted with a diamond cutting disc, followed by cold mounting of the samples in EpoFix resin. Subsequently, the mounted samples were successively ground and polished using Tegramin-25 equipment and SiC papers with grain sizes ranging from 220 to 4000 FEPA. This was followed by finer polishing using a composite disc and a 9-µm diamond paste. Further polishing was carried out with a "Dur" disc, using a 3-µm diamond suspension and a non-water-based lubricant to prevent corrosion of the Mg alloy. The sample was then subjected to additional polishing using a "Nap" disc with a 1-µm diamond paste.

EVO MA 15 electron microscope (Zeiss, Germany) was used to capture cross-section images of the specimen microstructure. For easier identification of different phases and determination of the coating and substrate materials and interfaces, the imaging was conducted in back-scattered electrons mode (BSE), sensitive to the element atomic weight. A relatively short work distance of 7–8 mm was employed to improve the yield and the contrast.

3.3.2 Porosity measurement in ImageJ

To measure the internal porosity of both Ti and HA coatings, image analysis was conducted using ten SEM images captured at random locations and identical magnification. The images were converted to 8-bit depth and gray contrast, and then manually thresholded using ImageJ software (NIH, USA) to differentiate the pores from particles. The threshold limits were set to correspond with the contrast of the pores. An illustration of the thresholding process is shown in Figure 22.

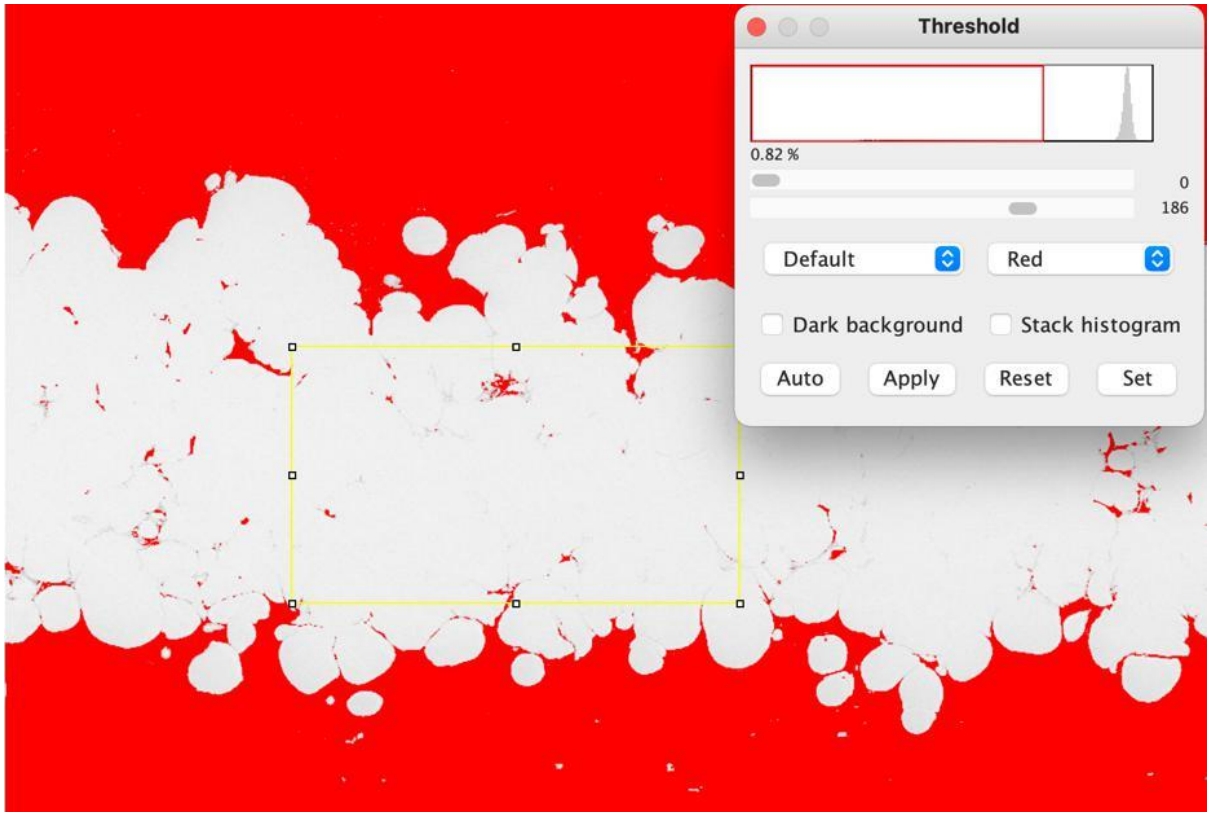

Figure 22: Porosity measurement in the ImageJ software, thresholding procedure.

3.3.3 Chemical composition and mapping

EDX mapping and area analysis of elemental distribution within the Ti/HA coating and AZ31 substrate as well as within the control HA coating on the Ti6Al4V substrate was conducted at low SEM magnifications to increase data reliability. Subsequently, a mapping of the elemental distribution was conducted near the coating-substrate interface at a higher magnification for extended times to provide more detailed information on local homogeneity. Last, a spectral line analysis was recorded across both interfaces to gain a more detailed look on the concentration profile of the individual elements in the coatings and the substrate.

4 Results and discussion

In this chapter, we will present and discuss the results of various analyses conducted on the hybrid Ti/HA coating deposited using a combination of cold spray and WSP-H spray techniques. These analyses include microstructural characterization using SEM and EDX, as well as internal porosity measurements using image analysis. The findings from these analyses will provide insight into the coating's quality, porosity, and composition, and will contribute to a better understanding of the feasibility of using this hybrid coating concept for biomedical applications of Mg alloys.

4.1 Results

4.1.1 Cold sprayed Ti microstructure

The SEM images presented in Figure 23 reveal a highly dense and homogeneous structure with a visible, but not very extensive degree of plastic deformation. At the interface, the titanium particles were embedded into the substrate with little to no visible plastic deformation (Figure 24). The surface is very coarse but its waviness is minimal. The thickness of the layer was measured at approximately 200 microns.

The microstructure exhibits a low porosity of only 0.6 % (measured from a set of 10 images), indicating the high density and compactness of the cold sprayed coating. Individual particles are tightly packed with barely visible boundaries between them.

However, a few oxidized regions on the particle boundaries can be observed as dark gray areas in the image. These localized oxidized regions are the remains of thin oxide layers that are inevitably present on the surface of the particles. Despite these oxidized regions, the overall microstructure remains predominantly dense and homogeneous.

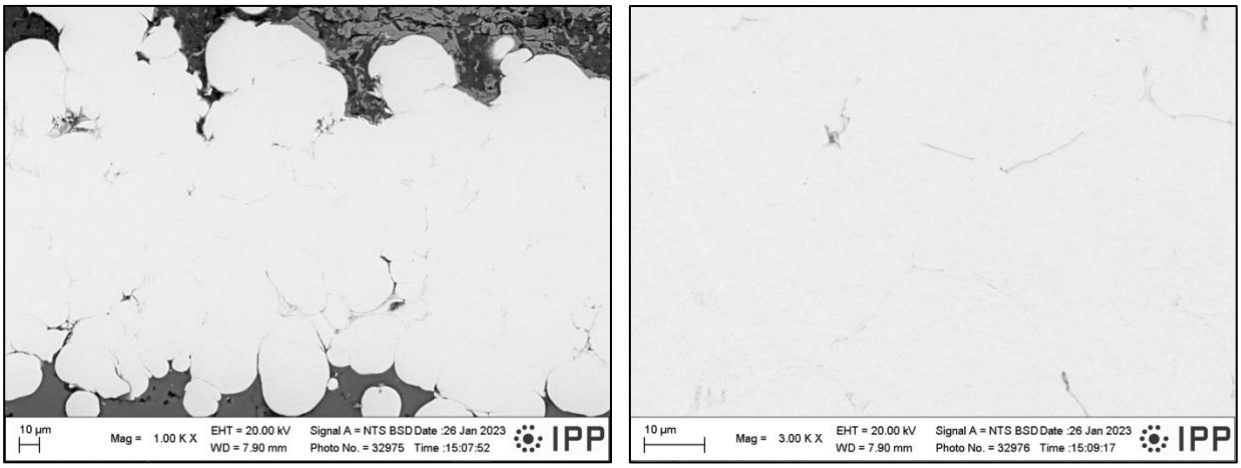

Figure 23: Cold sprayed Ti microstructure.

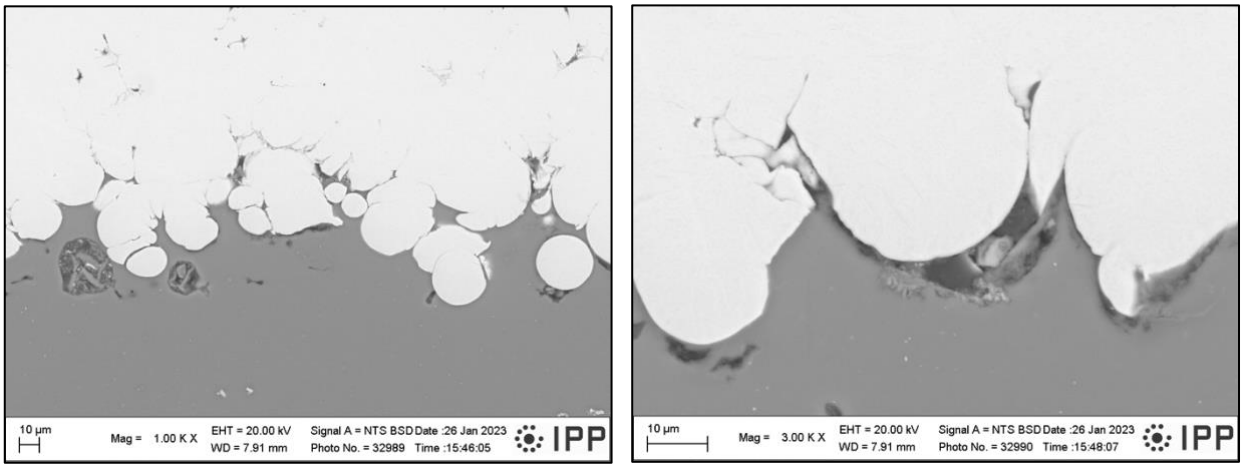

Figure 24: AZ31/Cold sprayed Ti interface.

4.1.2 WSP-H on CS microstructure

The WSP-H sprayed HA coating exhibits a splat structure with well-molten splats with significant agglomeration of molten primary particles, as is commonly observed in plasma-deposited materials (Figure 25). This structure arises from the rapid solidification of molten droplets upon impact, resulting in flattened and elongated shapes with occasional unmolten feedstock particles. Notably, the absence of through-thickness pores indicates a dense and protective coating that effectively shields the underlying Ti inter-layer and the AZ31 substrate. At the interface, the molten particles consolidated into the rough surface of the cold sprayed Ti coating (Figure 26).

Furthermore, the SEM images reveal the presence of columnar protrusions within the coating. These columnar structures are primarily formed on top surface irregularities of the underlying cold sprayed Ti coating and are a distinctive feature associated with spraying from a liquid feedstock.

The thickness is between 170–260 µm and the porosity reached an average value of 11.6 %.

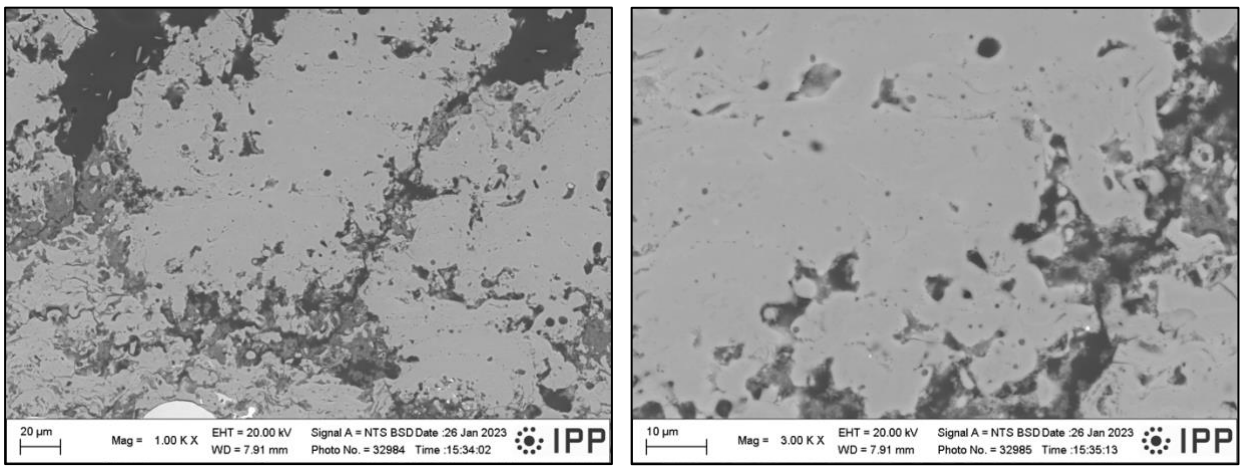

Figure 25: Plasma sprayed HA coating microstructure.

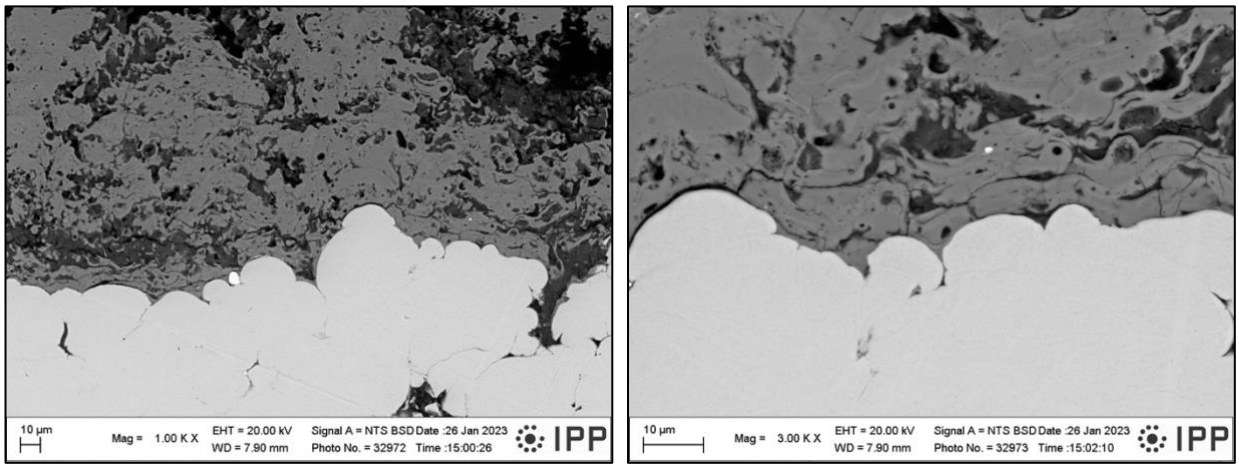

Figure 26: Cold sprayed Ti/Plasma sprayed HA interface.

4.1.3 WSP-H on Ti6Al4V microstructure

This control sample was prepared to determine whether the hydroxyapatite coating will produce coatings of similar properties to those deposited on pure titanium deposited using cold spray technology. We observed partial substrate melting of the substrate at the interface (Figure 28). Particles consolidated into surface irregularities of the substrate and formed a flat base coating. Similarly to the HA coating deposited on cold sprayed pure titanium, a columnar structure grew from the underlying flat part of the coating (Figure 27). One notable difference to the HA coating on the CS Ti is that the columnar protrusions seem to have grown under an angle. The porosity averages around 12%, which is comparable to the porosity observed in the HA coating on cold sprayed titanium.

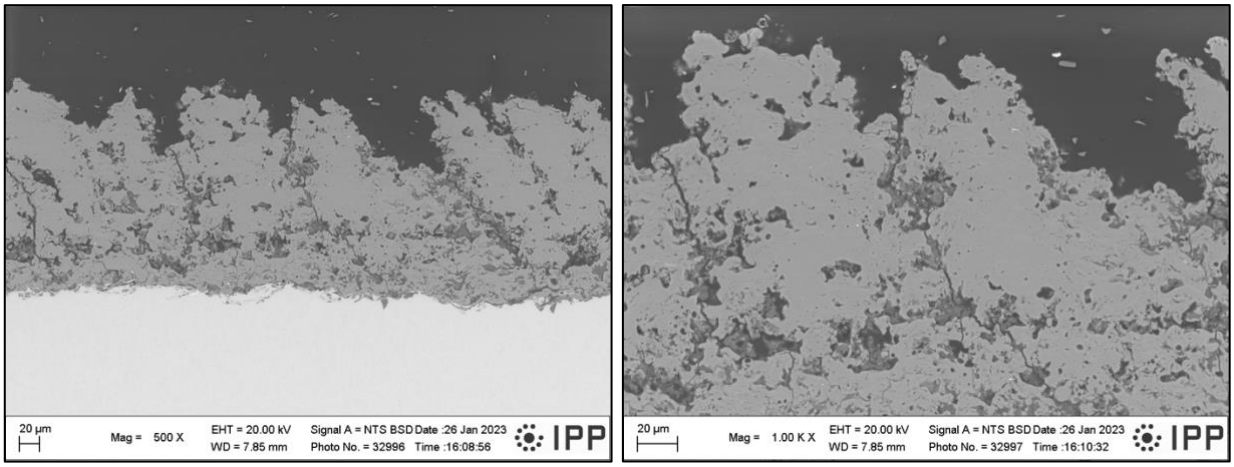

Figure 27: Ti6Al4V/Plasma sprayed HA microstructure.

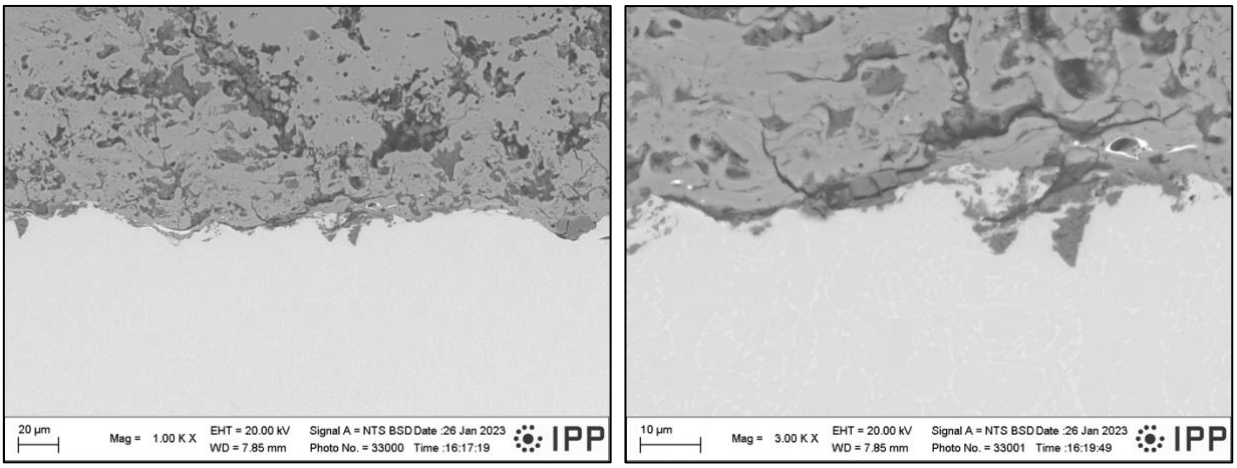

Figure 28: Ti6Al4V/Plasma sprayed HA interface.

4.1.4 Microstructure of the composite coating

As shown in Figure 29, the deposition of the hybrid coating was successful. The cold kinetic spray coating shows no signs of delamination from the magnesium substrate along its entire length, as does the HA topcoat on the CS Ti. The waviness of the coating is minimal, and the observed porosity appears to be low. The cohesion of cold sprayed base coat and plasma spray also appears to be satisfactory, as the hydroxyapatite particles have effectively consolidated within the surface irregularities of the titanium coating, forming a mechanical bond. The overall thickness of the hybrid coating ranges between 370 and 560 microns.

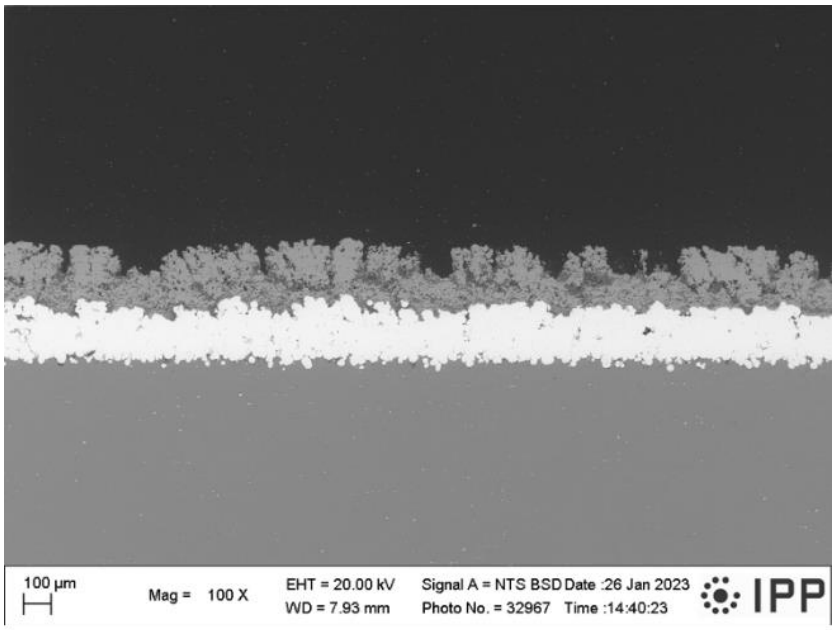

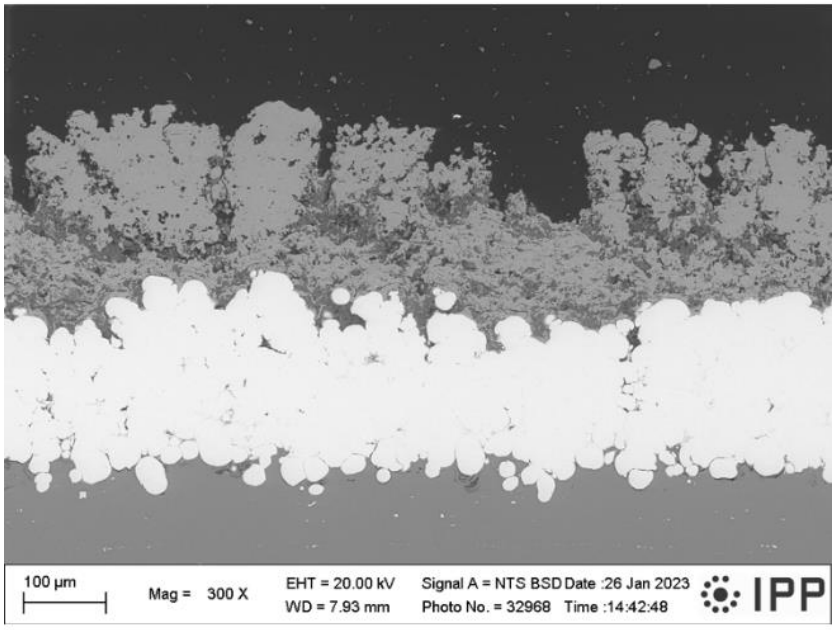

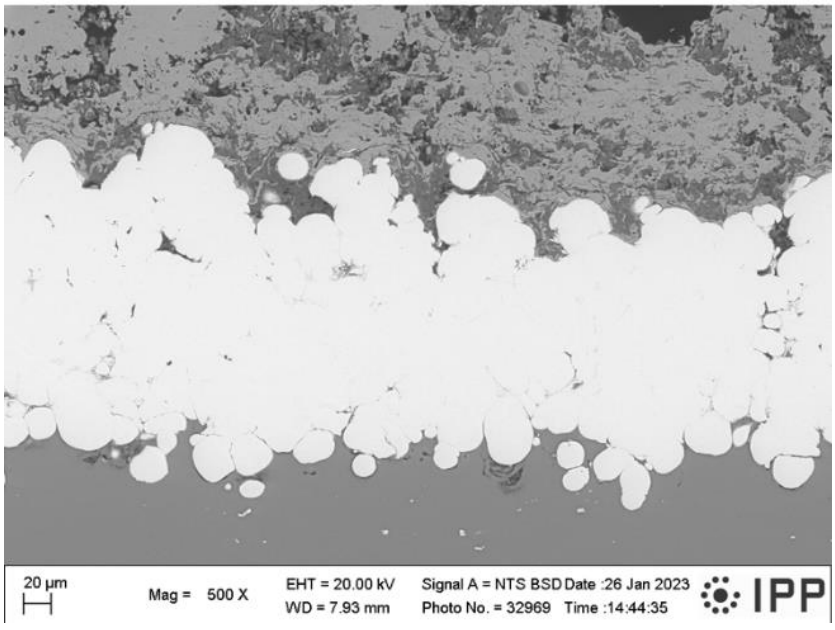

Figure 29: Composite CS Ti/WSP-H HA coating microstructure.

4.1.5 Chemical composition of the composite coating

The EDX mapping was performed to analyze the elemental distribution within the hybrid cold sprayed/plasma sprayed coating (Figure 31). Magnesium is predominantly observed within the AZ31 substrate, which contains aluminum-rich precipitates visible in the microstructure (Figure 18). Titanium is concentrated within the cold sprayed coating, with faint traces found at both the AZ31 and the HA in the vicinity of both interfaces. Calcium and phosphorus both display an even distribution within the plasma sprayed HA coating, subtly extending their presence to the cold sprayed Ti coating. Zinc is predominantly situated in the substrate, with a minor presence detected within the cold sprayed coating. Lastly, oxygen is present within the HA coating, but not in the CS Ti coating.

Furthermore, line spectra and EDX mapping were measured across both interfaces: AZ31/Ti, Ti/HA, and Ti6Al4V/HA in the control sample (see Figure 30, Figure 32, Figure 33 and Figure 34).

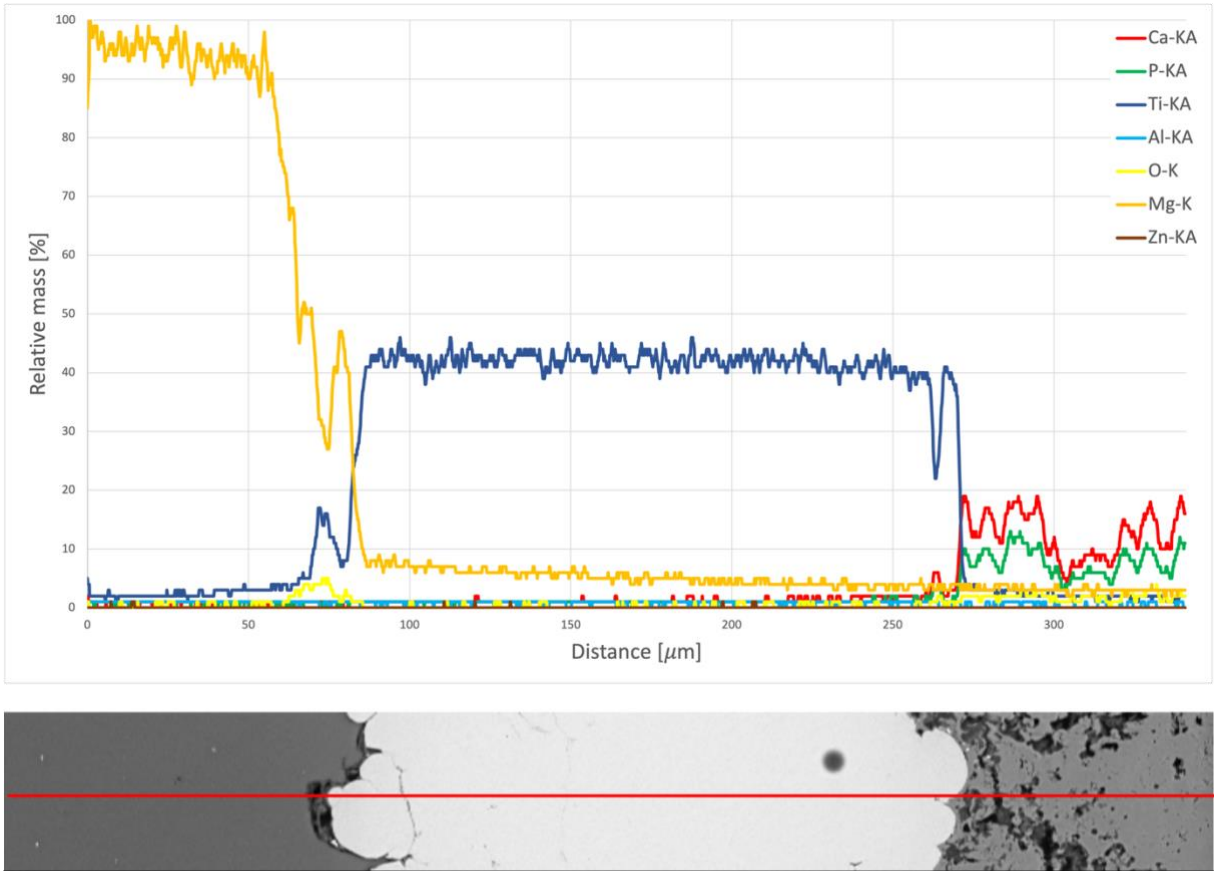

Figure 30: Line spectrum of both interfaces.

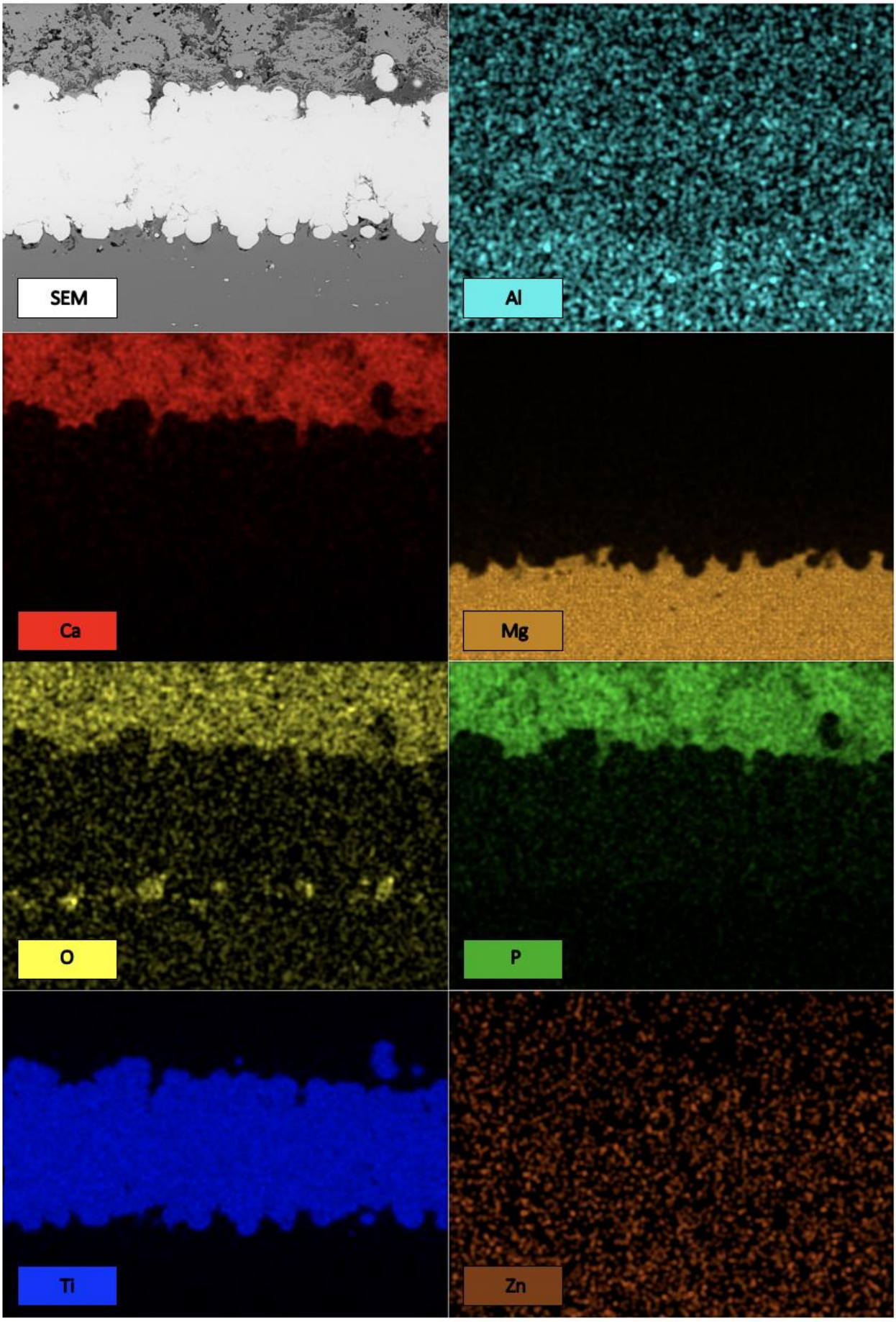

Figure 31: EDX elemental mapping of both interfaces.

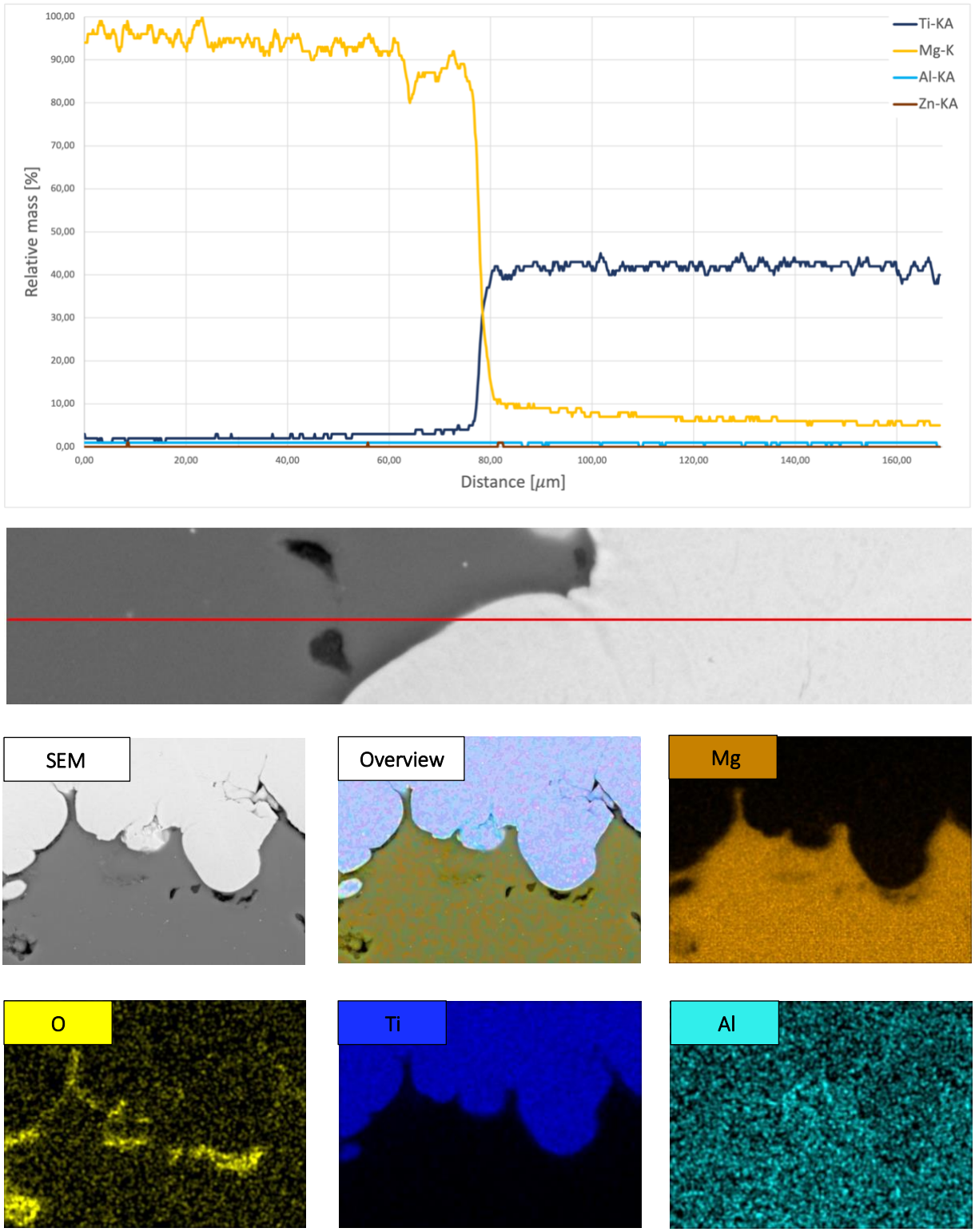

Figure 32: Line spectrum and EDX mapping of AZ31/Ti interface.

At the interface of AZ31 and Ti, a discontinuous transition between the main elements, titanium and magnesium, is observed (Figure 32). Some oxidation is visible at the boundary of the two materials.

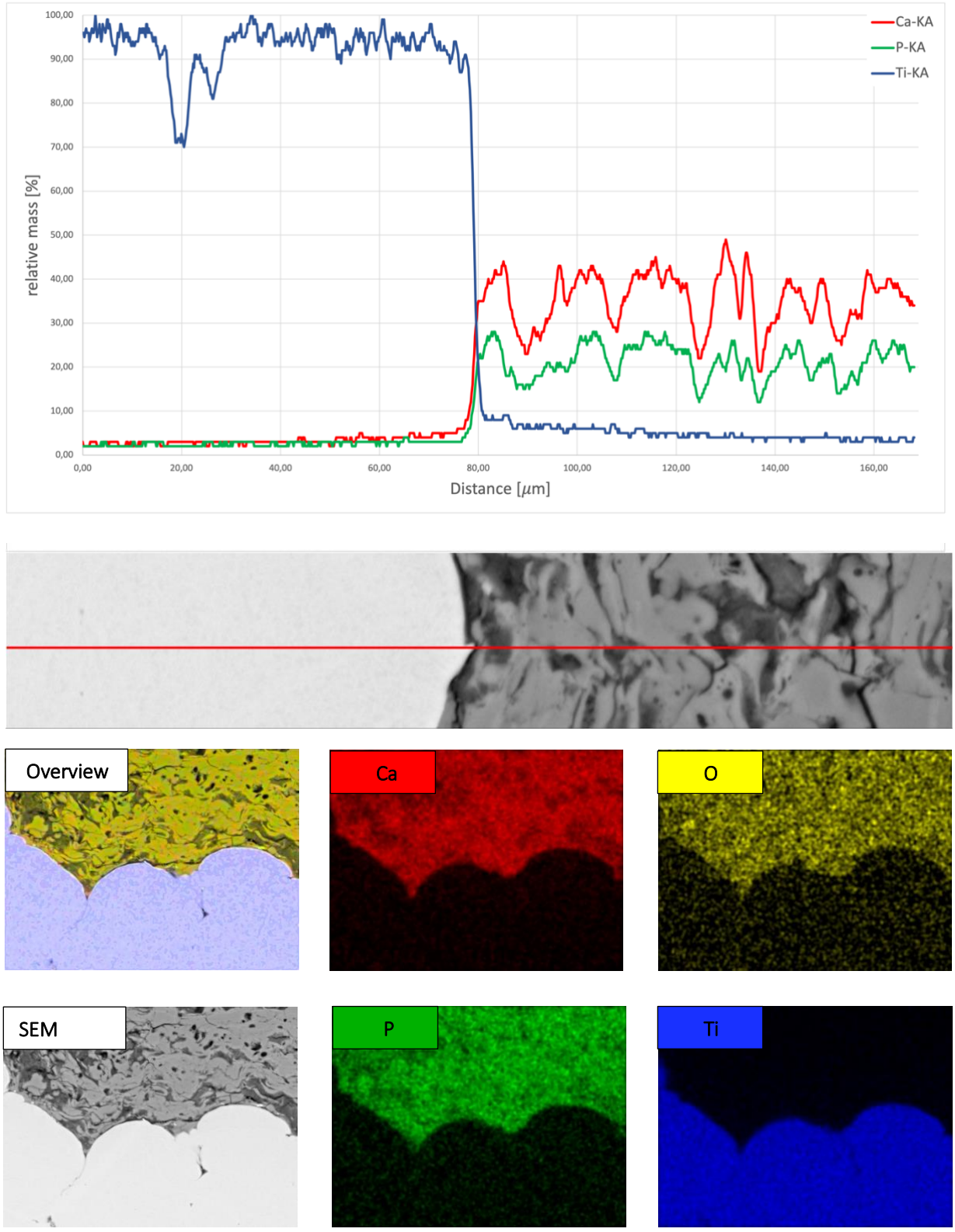

Figure 33: Line spectrum and EDX mapping of Ti/HA interface.

At the interface of Ti/HA, a similar phenomenon is observed, characterized by a sharp transition between the two layers. Titanium concentration gradually decreases after the transition into the HA layer.

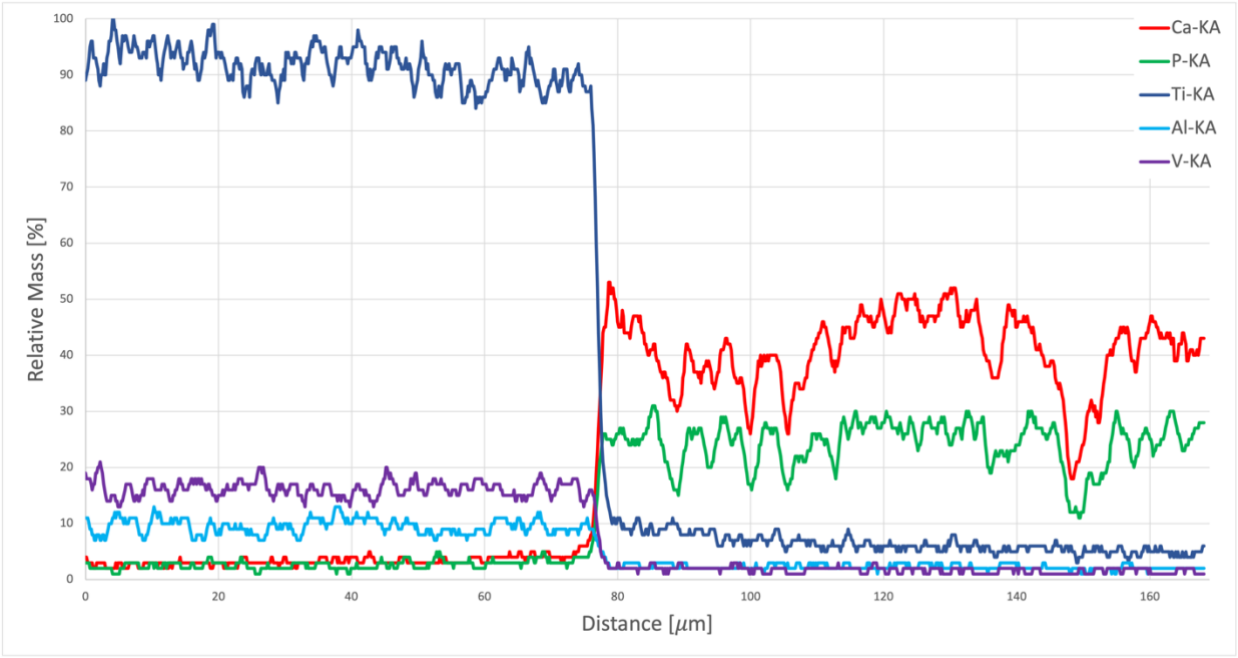

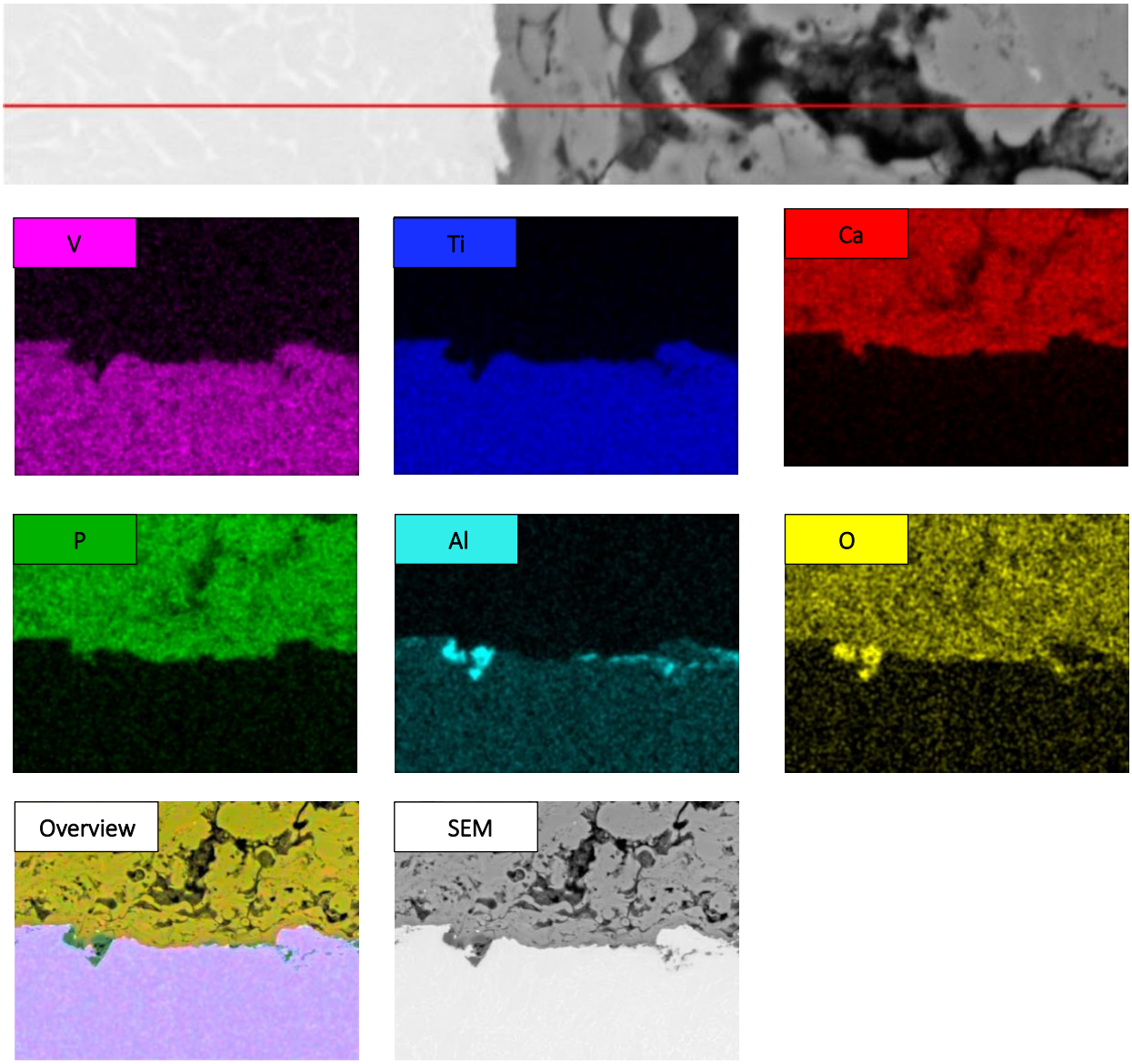

Figure 34: Line spectrum and EDX mapping of Ti6Al4V/HAp interface.

The hydroxylapatite coated Ti6Al4V sample also shows abrupt change in the chemical composition at the interface. Interestingly, while the aluminum and vanadium content drops to zero immediately after the transition from Ti6Al4V to HA, titanium content seems to decrease linearly after the initial drop in concentration. This effect was also observed at the pure Ti/HA interface.

4.2 Discussion

There are compelling reasons for using Mg alloys as replacements for hard tissues, such as their low modulus (see section 2 for a detailed explanation). However, a surface coating is necessary in order to prevent any dissolution of unwanted elements into the surrounding environment as well as increase the biocompatibility of the implant. The surface coating requirements for magnesium alloys are so diverse a single coating could barely meet them. Therefore, we have decided to address the requirements through a hybrid coating approach utilizing two different technologies. The first, cold sprayed titanium coating aims to protect and isolate the used Mg alloy AZ31 from the external environment, while the second, suspension plasma sprayed hydroxylapatite coating ensures biocompatibility and better bone integration.

The cold spray process demonstrated a remarkable efficiency in achieving a substantial coating thickness in a very short time span. With only four torch passes, the desired thickness of 200 microns was attained, requiring only a few seconds of spraying. This notable advantage sets cold spray apart from other processes like PVD or CVD, where typical maximum thicknesses are limited to the order of microns.

Equally significant is the absence of any coating delamination observed throughout the entire length of the sample. This indicates excellent adhesion and good interparticle contact, which can be attributed to the mechanical interlocking and metallurgical bonding between the two metals, result of two out of the three bonding mechanisms in cold spray.

Notably, the first layer of Ti particles did not undergo significant deformation, in contrast to the typical flattening observed in cold spray deposits [50]. This outcome can be attributed to the relatively low hardness of the Mg-based substrate material used in this study [17]. Here, it is worth mentioning that cold spray technology is widely recognized for its ability to deposit coatings even on soft substrates, including polymers.

The microstructure of the CS Ti is characterized by a tightly interconnected network of particles with a porosity of only 0.5%, setting it apart from other thermal spray techniques. In this structure, individual particles are barely discernible, displaying only subtle contours. Interestingly, the degree of particle deformation was relatively low. This could be attributed to the parameters used for the deposition (45 bar and 700 °C of the nitrogen gas). Further improvement could be made by raising the pressure to 50 bars and the temperature to 1100 °C [51].

Even with a significant coating thickness, no segmentation cracks are observed—a common occurrence in coatings produced by alternative thermal spray deposition methods. In these methods, the cracks typically result from quenching stresses associated with the phase change from liquid droplets to solid splats, as well as thermal contraction following deposition, caused by the coefficient of thermal expansion (CTE) mismatch between the coating and the substrate.

The titanium coating is very pure, with only slightly visible diffusion of magnesium. In other words, diffusion probably occurred during the cold spraying process to some extent. But since Mg is visible over virtually the entire thickness of the titanium coating, the diffusion most likely continued during the high heating of the sample during the subsequent plasma spraying process too. Another traceable element is oxygen, that is inevitably present as a very thin film on the surface of the atomized titanium particles and its content was therefore inherited into the cold sprayed Ti coating. The oxygen content can be mostly visible as the dark-contrast contours between the individual particles.

The waviness of the coating was minimal due to well optimized overlap parameter. The surface of the Ti coating is very irregular and rough, which helps consolidate the subsequent plasma sprayed coating and thus improves adhesion.

At the interface between the plasma sprayed hydroxyapatite and cold-sprayed Ti coatings, partially molten titanium particles are visibly present due to the high temperatures involved in the plasma spray process, reaching several thousand degrees Celsius. This occurrence is attributed to the thermal energy imparted during the process. This confirms the need to apply a titanium coating first, as it will protects the magnesium substrate not only from the biological effects of the surrounding tissue, but also from the extreme thermal loading during the plasma spray deposition of hydroxyapatite. Also, some diffusion of titanium into hydroxylapatite took place, since the line spectral analysis shows its concentration to decrease linearly instead of a sharp drop to zero, as was the case with aluminum and vanadium in the control sample.

The plasma sprayed HA coating exhibits a thickness ranging from 170 to 280 microns, which exceeds the optimal range (20-160 microns [3]) for our specific application, potentially leading to delamination issues. However, this issue can be easily resolved just by lowering the number of torch passes. The lower region of the coating interfacing with the CS titanium displays a typical splat-like structure commonly observed in plasma spraying processes. Although most of the individual splats seem to be well-melted and effectively bonded, some areas contain incompletely melted particles. This occurrence is likely attributed to incomplete fragmentation of the suspension upon entering the plasma jet. Some bigger droplets were not able to evaporate completely, which inhibited the proper melting of some of the particles.

From this lower flat region of the HA coating, a columnar structure emerges, a characteristic feature of coatings plasma sprayed from suspensions. This structure develops when utilizing suspensions containing nano-sized particles. The small particles exhibit a tendency to deviate laterally along with the gas flow at the substrate vicinity. This occurs when a certain coating thickness is reached, leading to a transition in the deposition mechanism to a "side-way" mode,

resulting in the formation of the columnar structure. In our composite coating, these structures originate from surface peaks on the cold sprayed Ti coating, as they are the first to pick up HA particles as they are swept to the side by the gas stream. Interestingly, on the control Ti6Al4V sample, the columns were angled at approximately 20 degrees, which was caused by the position of the sample on the holding carousel. The columns consist of agglomerated splats and exhibit a lower incidence of porosity compared to the part of the coating. However, the pores within the columns are relatively larger. While no horizontal cracks are apparent, numerous vertical cracks are observed in the columns. These cracks may arise from factors such as rapid cooling, hydroxyapatite crystallization, or excessive coating thickness.

From a chemical standpoint, the HA coating is composed of oxygen, phosphorus, calcium and hydrogen, with signs of diffusion originating from the underlying titanium layer. The theoretical ratio of Ca to P in HA is 10/6, which is equivalent to 1.67:1. In our coatings, we measured the ratio to be significantly higher, about 2.4:1. This may be caused by selective evaporation of phosphorus due to its low boiling point (300°C), as also shown in other studies [46]. In the linear chemical analysis, fluctuations in the signal intensity were observed for both Ca and P. However, these do not correspond to real lower concentrations of the two elements (Figure 33). Instead, this is attributed to poorly melted particles or porosity, which generates a weaker BSE signal in the SEM. The measured porosity of 11.6% is optimal for biological purposes, with no pores traversing the entire coating, indicating sufficient protection. As shown in a paper by Heimann [3], a higher porosity (5–20%) can enhance the adhesion of bone cells and facilitate tissue ingrowth into the implant, thereby increasing the chances of implant acceptance and establishing a stronger bone-implant interface.

In general, it can be said that a successful application of a composite coating on AZ31 substrate was achieved in this study. The resulting titanium cold spray layer exhibits characteristics suitable for the intended application, fulfilling the requirement of complete protection of the underlying magnesium alloy material against the surrounding environment. Subsequently, the hydroxyapatite layer applied via the WSP-H technique represents the first attempt of this kind. Despite its slightly higher thickness, the overall appearance of the hydroxyapatite coating is satisfactory, with no cracks extending through the entire cross-section, effectively isolating the underlying titanium and providing favorable conditions for future anchoring of cells and bone tissue growth.

5 Conclusions

The objective of this study was to assess the feasibility of fabricating a hybrid coating comprising of a base layer of titanium deposited via cold spraying and a top layer of hydroxylapatite sprayed from suspension using the WSP-H technology. The deposition was successful, and the resulting coating was evaluated for its potential as a surface treatment for next-generation implants.

The magnesium alloy AZ31 was chosen as the substrate due to its mechanical properties, specifically its resemblance to human bone in terms of the Young's modulus of elasticity. The cold spraying process employed pure titanium powder consisting of 100% alpha phase, while the plasma spraying technique utilized a 100% pure hydroxylapatite suspension produced in-house at the IPP facility.

From the obtained results, the following conclusions can be drawn:

- Titanium can be successfully deposited via cold spraying even on soft substrates such as magnesium when the process parameters are optimized, leading to the formation of a compact and characteristic microstructure.
- The intermediate titanium layer provides a sufficient thermal protection to the magnesium substrate during the deposition of hydroxyapatite via plasma spraying, preventing its degradation.
- A relatively thick hydroxyapatite coating can be successfully deposited onto the cold sprayed titanium layer without delamination issues.
- The chemical purity of both coatings remains largely preserved throughout the coating process. This holds also for the CS titanium that was subsequently exposed to the plasma spray process.

For future experiments, reducing the number of torch passes is recommended to lower the hydroxylapatite layer thickness to try reducing the vertical cracking extent. Furthermore, a tailored optimization of the spraying parameters for the titanium coating is advisable to prevent the occurrence of horizontal cracks that may potentially result in complete delamination of the layer.

Following improvements to the properties of the hydroxyapatite layer, subsequent biocompatibility tests will be carried out in a close collaboration at University of Hong Kong. This includes immersion in Hank's solution and monitoring the behavior of the hydroxyapatite layer, conducted to assess its interaction with the biological environment.

6 List of figures

7 List of tables

8 Literature

[1] VILARDELL, A. Martín; CINCA, Nuria; CONCUSTELL, Amadeau. Cold spray as an emerging technology for biocompatible and antibacterial coatings: state of art. Journal of Materials Science, 2015, 50: 4441-4462., p. 4441–4462..

[2] THAMARAISELVI, T.; RAJESWARI, S. Biological evaluation of bioceramic materials-a review. Carbon, 2004..

[3] HEIMANN, Robert B. Plasma-sprayed hydroxylapatite-based coatings: chemical, mechanical, microstructural, and biomedical properties. Journal of Thermal Spray Technology, 2016..

[4] NIINOMI, Mitsuo. Biomedical titanium alloys with Young's moduli close to that of cortical bone. Regenerative biomaterials, 2016, 3.3: 173-185...

[5] EFREMENKO, V. G. Micromechanical, corrosion and wet sliding wear behaviours of Co-28Cr-6Mo alloy: Wrought vs. LPBF. Materials Today Communications, 2023..

[6] ZENG, Rongchang, et al. Progress and challenge for magnesium alloys as biomaterials. Advanced engineering materials, 2008, 10.8: B3-B14...

[7] SEZER, Nurettin, et al. Review of magnesium-based biomaterials and their applications. Journal of magnesium and alloys, 2018, 6.1: 23-43...

[8] WALKER, Jemimah; SHADANBAZ, Shaylin; DIAS, J. George. Magnesium biomaterials for orthopedic application: A review from a biological perspective..

[9] HENCH, Larry L. Biomaterials: a forecast for the future. Biomaterials, 1998, 19.16: 1419-1423., vol. 19.16, pp. 1419-1423..

[10] GRUJICIC, Mica. Analysis of the impact velocity of powder particles in the cold-gas dynamic-spray process. Materials Science and Engineering: A, 2004..

[11] WU, Guosong; IBRAHIM, Jamesh Mohammed; CHU, Paul K. Surface design of biodegradable magnesium alloys—A review. Surface and Coatings Technology, 2013, 233: 2-12., vol. 220, pp. 60-66..

[12] BINYAMIN, Gary; SHAFI, Bilal M.; MERY, Carlos M. Biomaterials: a primer for surgeons. In: Seminars in pediatric surgery. WB Saunders, 2006..

[13] DAROONPARVAR, Mohammadreza, et al. Improvement of wear, pitting corrosion resistance and repassivation ability of mg-based alloys using high pressure cold sprayed (HPCS) commercially pure-titanium coatings. Coatings, 2021..

[14] VILARDELL, A. Martín, et al. Cold spray as an emerging technology for biocompatible and antibacterial coatings: state of art. Journal of Materials Science, 2015, 50: 4441-4462., p. 4441–4462..

[15] Cold spray gun by impact innovations, 2023. Impact innovations GmbH [online]. Cit. [2023-08-05]. Available from: https://impact-innovations.com/en/portfolio-item/cold-spray-guns/..

[16] POZA, Pedro; GARRIDO-MANEIRO, Miguel Ángel. Cold-sprayed coatings: Microstructure, mechanical properties, and wear behaviour. Progress in Materials Science, 2022, 123: 100839., vol. 123..

[17] SINGH, Surinder, et al. Influence of cold spray parameters on bonding mechanisms: A review. Metals, 2021, 11.12: 2016...

[18] GRUJICIC, Mica. Adiabatic shear instability based mechanism for particles/substrate bonding in the cold-gas dynamic-spray process. Materials & design, 2004..

[19] JOSHI, Aneesh; JAMES, Sagil. Molecular dynamics simulation study of cold spray process. Journal of Manufacturing Processes, 2018, 33: 136-143...

[20] HASSANI-GANGARAJ, Mostafa. Adiabatic shear instability is not necessary for adhesion in cold spray. Acta Materialia, 2018..

[21] ASSADI, Hamid; KREYE, Heinrich; KLASSEN, Thomas. Cold spraying–A materials perspective. Acta Materialia, 2016, 116..

[22] SCHMIDT, Tobias, et al. Development of a generalized parameter window for cold spray deposition. Acta materialia, 2006, 54.3: 729-742...

[23] ROKNI, M. R., et al. Review of relationship between particle deformation, coating microstructure, and properties in high-pressure cold spray. Journal of thermal spray technology, 2017, 26: 1308-1355...

[24] KOIVULUOTO, Heli, et al. High pressure cold sprayed (HPCS) and low pressure cold sprayed (LPCS) coatings prepared from OFHC Cu feedstock: overview from powder characteristics to coating properties. Journal of thermal spray technology, 2012, 21: 1065-1075..

[25] AKEDO, Jun. Room temperature impact consolidation (RTIC) of fine ceramic powder by aerosol deposition method and applications to microdevices. Journal of Thermal Spray Technology, 2008, 17..

[26] BHATTIPROLU, Venkata Satish, et al. Influence of feedstock powder and cold spray processing parameters on microstructure and mechanical properties of Ti-6Al-4V cold spray depositions. Surface and Coatings Technology, 2018..

[27] PRASAD, K., et al. Printability of low-cost pre-heat-treated ball milled Al7075 powders using compressed air assisted cold spray additive manufacturing. Additive Manufacturing Letters, 2022, 3: 100046...

[28] YANG, Guan-Jun, et al. Mechanical property and wear performance dependence on processing condition for cold-sprayed WC-(nanoWC-Co). Applied Surface Science, 2015, 332: 80-88...

[29] SNGH, Reeti, et al. High-performance Cold Spray Coating for Wear/Corrosion Protection and Particle Emission Reduction of Brake Discs. In: International µ-Symposium Brake Conference. Berlin, Heidelberg: Springer Berlin Heidelberg, 2022..

[30] SUN, Wen, et al. Current implementation status of cold spray technology: A short review. Journal of Thermal Spray Technology, 2022..

[31] MORIDI, Atieh, et al. Solid-state additive manufacturing of porous Ti-6Al-4V by supersonic impact. Applied Materials Today, 2020..

[32] CHAMPAGNE, V.; HELFRITCH, D. Critical Assessment 11: Structural repairs by cold spray. Materials Science and Technology, 2015..

[33] NASA additively manufactured rocket engine hardware. [online]. Available from: https://www.nasa.gov/centers/marshall/news/releases/2021/nasa-additively-manufactured-rocket-engine-hardware-passes-cold-spray-hot-fire-tests.html.

[34] LASHMI, P. G., et al. Present status and future prospects of plasma sprayed multilayered thermal barrier coating systems. Journal of the European Ceramic Society, 2020, 40.8: 2731-2745., vol. 40, pp. 2731-2745..

[35] DAVIS, J.R. Handbook of thermal spray technology. Materials Park, OH: ASM International, 2004..

[36] MATĚJÍČEK, Jiří; KOZA, Yoshie; WEINZETTL, Vladimír. Plasma sprayed tungsten-based coatings and their performance under fusion relevant conditions. Fusion engineering and design, 2005, 75: 395-399., vol. 85, pp. 1521-1526..

[37] HRABOVSKÝ, Milan, et al. Properties of water stabilized plasma torches. Thermal Plasma Torches and Technologies, 2000, 1: 242-266...

[38] HRABOVSKY, Milan. Generation of thermal plasma jets in liquid-stabilized and hybrid gas-liquid plasma torches. In: Proceedings of DAE-BRNS symposium on applications of plasmas, lasers and electron beams in advanced materials processing. 2002...

[39] ODHIAMBO, John Gerald, et al. Porosity and its significance in plasma-sprayed coatings. Coatings, 2019, 9.7: 460...

[40] VETRIVENDAN, E., et al. Argon shrouded plasma spraying of tantalum over titanium for corrosion protection in fluorinated nitric acid media. Journal of Thermal Spray Technology, 2018, 27: 512-523...

[41] ROTH, J. Reece. Industrial plasma engineering: Volume 2: Applications to nonthermal plasma processing. CRC press, 2001., p. 39..

[42] GUIPONT, V. High-pressure plasma spraying of hydroxyapatite powders. Materials Science and Engineering: A, 2002..

[43] XIAO, Lisong, et al. Nanostructured TiN coating prepared by reactive plasma spraying in atmosphere. Applied Surface Science, 2007, 253.18: 7535-7539...

[44] NOURI, Alireza; SOLA, Antonella. Powder morphology in thermal spraying. Journal of Advanced Manufacturing and Processing, 2019, 1.3: e10020...

[45] VAßEN, Robert, et al. Suspension plasma spraying: process characteristics and applications. Journal of thermal spray technology, 2010.

[46] CIZEK, Jan; CHRASKA, Tomas; LUKAC, Frantisek. Silver-doped hydroxyapatite coatings deposited by suspension plasma spraying. Journal of Thermal Spray Technology, 2018..

[47] JOSHI, Shrikant; NYLEN, Per. Advanced coatings by thermal spray processes. Technologies, 2019, 7.4: 79...

[48] SMITH, M. F. Comparing cold spray with thermal spray coating technologies. In: The cold spray materials deposition process. Woodhead Publishing, 2007. p. 43-61...

[49] Hybrid WSP-H plasma technology, 2023. IPP CAS [online]. Cit. [2023-15-05]. Available from: https://www.wsp-h.com/..

[50] LI, Wenya; CAO, Congcong; YIN, Shuo. Solid-state cold spraying of Ti and its alloys: A literature review. Progress in Materials Science, 2020..

[51] CIZEK, J., et al. Measurement of mechanical and fatigue properties using unified, simple-geometry specimens: Cold spray additively manufactured pure metals. Surface and Coatings Technology, 2021..

[52] Titanium dental implant, 2023. In: Toner family dentistry [online]. cit. [2023-08-05]. Available from: https://www.tonerfamilydentistry.com/implants..

[53] WALKER, Michael. Microstructure and bonding mechanisms in cold spray coatings. Materials Science and Technology, 2018, 34.17: 2057-2077., vol. 34, pp. 2057-2077..

[54] OLAKANMI, E. O.; DOYOYO, M. Laser-assisted cold-sprayed corrosion-and wear-resistant coatings: a review. Journal of thermal spray technology, 2014, 23: 765-785...

[55] JEN, Tien-Chien, et al. The acceleration of charged nano-particles in gas stream of supersonic de-Laval-type nozzle coupled with static electric field. Applied thermal engineering, 2006, 26.5-6: 613-621...

[56] SINGH, Harvinder; KUMAR, Manoj; SINGH, Rajdeep. An overview of various applications of cold spray coating process. Materials Today: Proceedings, 2022, 56: 2826-2830...

[57] WANK, A. Basics of thermal spray technology. GTV Verschleiss-Schutz GmbH: Luckenbach, Germany, 2006...

[58] MUSALEK, Radek, et al. Microstructures and thermal cycling properties of thermal barrier coatings deposited by hybrid water-stabilized plasma torch. Journal of Thermal Spray Technology, 2020, 29: 444-461., vol. 29, pp. 444-461..

[59] YIN, Shuo, et al. Formation conditions of vortex-like intermixing interfaces in cold spray. Materials & Design, 2021, 200: 109444., vol. 200..